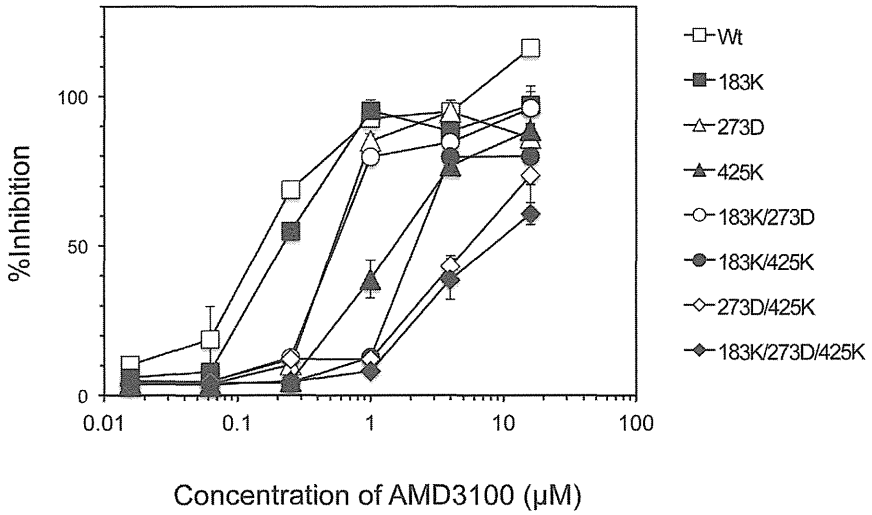


**Figure 4. Susceptibilities of replication-competent recombinant viruses.** SupT1/CCR5 cells were infected with the same amount of replication-competent recombinant viruses carrying mutations (100 $TCID_{50}$) in the presence of various concentrations of AMD3100, and then cultured for 6 days. Cytopathic effects were determined by an MTT assay. Data are the means ± SD of triplicate experiments.
doi:10.1371/journal.pone.0089515.g004

infectious molecular clones carrying single or multiple mutations. The sensitivity of each mutant was then determined by an MTT assay using SupT1/CCR5 cells (Fig. 4, Table 1). In single mutants, M425K and N273D conferred 10-fold and 3-fold reduced sensitivities to AMD3100, respectively, whereas N183K was almost dispensable. Furthermore, mutants carrying both N273D and M425K (N273D/M425 and N183K/N273D/M425K) conferred a more than 40-fold reduced sensitivity to AMD3100. To confirm the sensitivity of mutants to AMD3100 using a single-round entry assay, we constructed Env expression vectors carrying single or multiple mutations. Pseudotyped viruses carrying the luciferase gene were produced by cotransfection of 293T cells with these vectors and an *env*-lacking luciferase-reporter HIV-1 construct. The sensitivity of each mutant was then determined using NP2/CD4 cells expressing both CXCR4 and CCR5 (Table 2). In single mutants, N273D and M425K substitutions conferred reduced sensitivity to AMD3100 (4.1-fold and 2.6-fold, respectively), whereas N183K had a minor effect (1.5-fold) as shown in Table 2. The N293D mutation combined with M425K (273D/425K) conferred increased resistance to AMD3100 (10-fold). In contrast, addition of N183K had a minor effect on the reduced sensitivity to AMD3100 in combination with N273D/M425K (13-fold). These results indicated that both N273D and M425K were mainly involved in the reduced sensitivity to AMD3100. The reduced sensitivity to AMD3100 was thus independent of the V3 loop.

We next determined whether viruses carrying these mutations were cross-resistant to another CXCR4 inhibitor, T134 [24] (Table 2). We found that a single M425K mutation and combinations with M425K were cross-resistant to T134 (3-fold).

**Table 1.** Susceptibility of recombinant viruses to AMD3100 determined by MTT assays.

| virus | $EC_{50}$ (μM)[a] |
|---|---|
| | AMD3100 |
| wild type | 0.15±0.02[b](1.0) |
| 183K | 0.21±0.01 (1.5) |
| 273D | 0.52±0.02 (3.6) |
| 425K | 1.5±0.23(10) |
| 183K/273D | 0.54±0.01 (3.7) |
| 183K/425K | 2.2±0.05(14) |
| 273D/425K | 5.9±1.4(40) |
| 183K/273D/425K | 10.3±2.5(70) |

[a]SupT1/CCR5 cells ($5\times10^3$) were infected with 100$TCID_{50}$ recombinant viruses, and then the cytotoxicity induced by HIV-1 was measured at day 6 post-infection by an MTT assay to determine the effective concentration of 50% inhibition ($EC_{50}$).
[b]Mean ± SD (n = 3). Numbers in parenthesis represent fold changes of $EC_{50}$ values compared with that of the wild type.
doi:10.1371/journal.pone.0089515.t001

**Table 2.** Susceptibilities of recombinant pseudotyped viruses to CXCR4 inhibitors determined by single-round entry assays.

| virus | $EC_{50}$ (μM)[a] | | | |
|---|---|---|---|---|
| | AMD3100 | | T134 | |
| wild type | 0.012±0.0047[b] | (1.0) | 0.033±0.0086 | (1.0) |
| 183K | 0.018±0.0015 | (1.5) | 0.023±0.0064 | (0.7) |
| 273D | 0.052±0.029 | (4.1) | 0.034±0.0010 | (1.0) |
| 425K | 0.032±0.012 | (2.6) | 0.097±0.011 | (2.9) |
| 183K/273D | 0.031±0.015 | (2.4) | 0.054±0.014 | (1.6) |
| 183K/425K | 0.020±0.012 | (1.6) | 0.062±0.011 | (1.9) |
| 273D/425K | 0.12±0.014 | (10) | 0.061±0.013 | (1.8) |
| 183K/273D/425K | 0.16±0.031 | (13) | 0.099±0.013 | (3.0) |

[a]NP2/CD4/CXCR4/CCR5 cells ($1.5\times10^4$) were infected with pseudotyped virus (50 ng p24Ag) in the presence of CXCR4 inhibitors, and then the luciferase activity was measured at 48 h post-infection to determine the effective concentration of 50% entry inhibition ($EC_{50}$).
[b]Mean ± SD (n = 3). Numbers in parenthesis represent fold changes of $EC_{50}$ values compared with that of the wild type.
doi:10.1371/journal.pone.0089515.t002

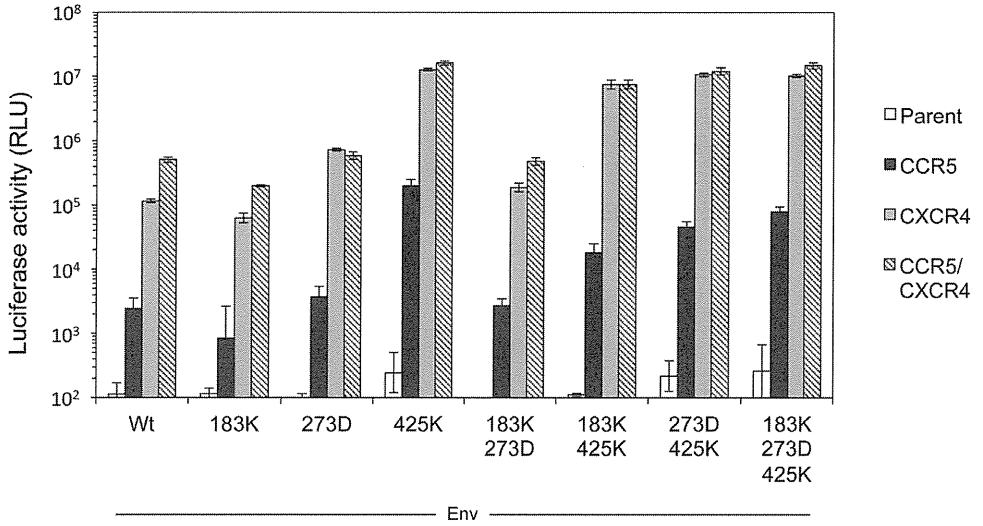


**Figure 5. Coreceptor usage and entry efficiency of recombinant pseudotyped HIV.** Coreceptor usage of the recombinant luciferase-reporter HIV was determined using NP2/CD4 cells expressing either CCR5 or CXCR4. Entry efficiencies of recombinant pseudotyped HIVs were determined using NP2/CD4 cells expressing both CXCR4 and CCR5. The cells were infected with the same amount of luciferase-reporter pseudotyped virus (10 ng p24Ag) with the indicated mutations. Luciferase activities were measured at 48 h post-infection. Data are the geometric means ± SD of triplicate experiments.
doi:10.1371/journal.pone.0089515.g005

However, similar to the wild-type, N273D was sensitive to T134.

## Involvement of the C4 region in enhanced replication of AMD3100-resistant HIV-1

We next evaluated whether these mutations changed the coreceptor preference from CXCR4 to CCR5. To this end, NP2/CD4 cells expressing either CCR5 or CXCR4 were infected with the luciferase-reporter HIV-1 pseudotyped with single or multiple mutations (Fig. 5). After infection of CXCR4-expressing cells with all recombinant viruses derived from JR-FLan/KI812.7, luciferase activities were ~100-fold higher than those of CCR5-expressing cells. This result indicated that all Envs, including N183K, N273D, and M425K, did not change preferential use of CXCR4. We also determined the entry efficiencies of the mutants using NP2/CD4 cells expressing both CXCR4 and CCR5. Luciferase activities of the cells infected with the same amount of the viruses (10 ng p24 Ag) showed that the single M425K substitution, but not N183K and N273D, increased the entry efficiency compared with that of the wild-type virus (Fig. 5). Mutations combined with 425K (183K/425K, 273/425K, and 183K/273D/425K) also had similar infectivities to that of the single mutation (Fig. 5), indicating that M425K substitution was

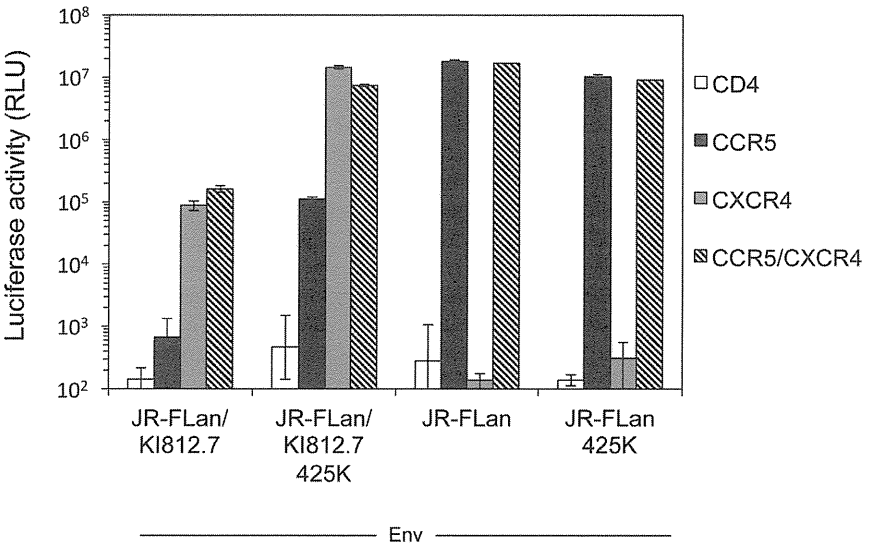


**Figure 6. Effect of M425K substitution on JR-FLan Env.** Coreceptor usage and entry efficiency of recombinant luciferase-reporter HIV pseudotyped with the indicated Envs were determined using NP2/CD4 cells expressing either CXCR4 or CCR5 and cells expressing both CXCR4 and CCR5, respectively. The cells were infected with the same amount of luciferase-reporter pseudotyped virus (10 ng p24Ag) with the indicated mutations. Luciferase activities were measured at 48 h post-infection. Data are the geometric means ± SD of triplicate experiments.
doi:10.1371/journal.pone.0089515.g006

**Table 3.** Susceptibility of recombinant pseudotyped viruses to sCD4 determined by single-round entry assays.

| virus | $EC_{50}$ (μg/mL)[a] |
|---|---|
| | sCD4 |
| wild type | >10 |
| 183K | >10 |
| 273D | 6.9±0.26[b] |
| 425K | 0.42±0.040 |
| 183K/273D | 8.6±0.89 |
| 183K/425K | 0.35±0.024 |
| 273D/425K | 0.14±0.0033 |
| 183K/273D/425K | 0.22±0.016 |

[a]NP2/CD4/CXCR4/CCR5 cells ($1.5\times10^4$) were infected with pseudotyped virus (50 ng p24Ag), and then the luciferase activity was measured at 48 h post-infection to determine the effective concentration of 50% entry inhibition ($EC_{50}$).
[b]Mean ± SD (n = 3).
doi:10.1371/journal.pone.0089515.t003

essential for enhancement of viral infectivity. We next determined whether the M425K substitution also enhanced the entry efficiency of JR-FLan Env. However, M425K substitution in JR-FLan Env neither increased the luciferase activity in NP2/CD4/CCR5/CXCR4 (Fig. 6) nor changed coreceptor usage from CXCR4 to CCR5. These results indicated that the enhanced infectivity by M425K substitution was only observed in the context of Env carrying the V3 loop from KI812.7.

### Involvement of C2 and C4 regions in the increased sensitivity to soluble CD4

Because the change in the C2 region (N273D) was located in loop D, which is associated with resistance to the monoclonal neutralizing antibody VRC01 and soluble (s)CD4 [40], we examined whether the mutations also affected the sensitivity to sCD4 (Table 3). We found that the wild-type virus was resistant to sCD4 (the $EC_{50}$ value was more than 10 μg/ml). N183K mutation did not change the sensitivity, whereas N273D increased the sensitivity to sCD4 to some extent ($EC_{50}$: 6.9±0.26 μg/mL). In contrast, M425K largely increased the sensitivity to sCD4 ($EC_{50}$: 0.42±0.04 μg/mL). These results indicated that not only the C2 mutation but also the C4 region mutation affected the increased sensitivity to sCD4.

## Discussion

Characterization of CXCR4 inhibitor-resistant HIV-1 is important to understand how the virus can escape from inhibitors targeting coreceptors although clinical application of CXCR4 inhibitors for treatment of HIV-1-infected individuals remains a matter of debate. In the present study, we successfully isolated an AMD3100-escape variant from dual-X4 HIV-1. Interestingly, the variants had substitutions in C2 and C4 regions (N273D and M425K, respectively), which were responsible for their resistance to AMD3100 based on site-directed mutagenesis experiments. In contrast, no remarkable changes were observed in the V3 loop. In general, the V3 loop is a crucial determinant for coreceptor selectivity and resistance to coreceptor inhibitors and natural ligands. CXCR4 inhibitor-resistant X4 viruses show numerous mutations in the V3 loop and other regions, although the responsible region(s) have mostly not been determined for the reduced sensitivity to CXCR4 inhibitors [24,25,26,27,28]. In our previous study, we also selected a CXCR4 inhibitor-escape variant from dual-X4 HIV-1, which had serine to arginine substitution at the 11th position of the V3 loop [30]. *In vitro* experiments have revealed that coreceptor selectivity of HIV-1 is determined by the amino acid sequence of gp120, particularly the number [41,42] and position of charged amino acids in the V3 loop such as the 11/25 rule. Thus, amino acid substitution in the V3 loop can predict the loss of CXCR4 usage. Indeed, mutational analysis confirmed reversion of dual-X4 to dual-R5 by substitution. Conversely, the dual-X4 virus used in this study did not have a positively charged amino acid at the 11th or 25th position of the V3 loop, such as arginine or lysine. However, the Geno2pheno coreceptor algorithm predicted CXCR4 use of this virus because of an increased net positive charge and lack of an N-linked glycan in the V3 loop. In fact, analyses of coreceptor usage revealed that the virus carrying the V3 loop from KI812.7 predominantly used CXCR4 as the coreceptor. Furthermore, the AMD3100-escape variant was found to predominantly use CXCR4 without reversion from CXCR4 to CCR5. Therefore, it is likely that viruses not carrying a charged amino acid at the 11th position of the V3 loop lose their ability to revert from CXCR4 to CCR5 use. To acquire resistance to CXCR4 inhibitors, such viruses may need to induce substitutions in the V3 loop or different regions of gp120, such as C2 and C4 regions.

It has been suggested that CXCR4 inhibitor-resistant viruses exhibit reduced fitness [25], probably because of lower affinity of gp120 for CXCR4. Notably, M425 is located in the β21 sheet of the gp120 bridging sheet that is thought to be important for coreceptor binding together with the stem of the V3 loop (V3 stem) [43,44,45]. Because there was no reduction in the maximum plateau inhibition [18] for AMD3100 in this escape variant, it is unlikely that the selected virus recognized the AMD3100-bound form of CXCR4 [46]. Instead, sufficient concentrations of AMD3100 reached~100% inhibition of the selected virus (right shift in the $EC_{50}$ value), indicating competitive resistance. It is thus possible that the M425K substitution may alter the binding affinity for CXCR4 in the context of the V3 loop from KI812.7 [47,48,49] to retain the viral replication fitness. Indeed, the M425K substitution was cross-resistant to another CXCR4 inhibitor, T134, and dramatically enhanced the entry efficiency of the virus carrying the V3 loop from KI812.7 (~100-fold) but not from the JR-FLan background. Other studies have also shown that escape from the CCR5 inhibitor vicriviroc is not associated with a loss of fitness [50], which is not caused by changes in the V3 loop, similar to our variant, but rather substitutions in the fusion peptide domain of gp41 [51]. Taken together, it is possible that coreceptor inhibitor-resistant viruses need to retain or increase the affinity for their coreceptors by changing V3 or non-V3 regions, which are probably dependent on the configuration of the V3 loop.

In contrast, the N273D substitution was also shown to be an important determinant for reduced sensitivity to AMD3100, although the mutation did not significantly increase the entry efficiency of the virus. In fact, N273D is located in loop D of the C2 region and is associated with the loss of N-glycan, indicating alteration of the whole structure of gp120 via steric hindrance. It has been shown that N273A affects sensitivities to the broadly neutralizing monoclonal antibody VRC01 and sCD4 [40]. The structure of VRC01 in complex with the gp120 core revealed that the VRC01 heavy chain binds to the gp120 CD4bs in a manner similar to that of CD4 [52]. Indeed, our mutations, not only N273D but also M425K, conferred sensitivity to sCD4, suggesting that these substitutions affect the CD4 binding affinity. It has been reported that AMD3100 directly interacts with $Asp^{171}$ and $Asp^{262}$

of CXCR4 [53], as well as ECL2 and TM4 [54]. However, inhibitory activities of AMD3100 in CXCR4 mutants at these positions are dependent on the strain of CXCR4-using HIV-1 [53]. Thus, different CXCR4-using HIV-1s vary in their dependence on residues in one or the other domains [55]. Taken together, it is possible that gp120 with N273D or M425K might recognize a different portion of the CD4/CXCR4 complex and alter their affinity. However, structural analysis of the gp120 core carrying these mutations with the V3 loop from KI812.7 is necessary to address these issues.

In conclusion, it is possible to induce a CXCR4 inhibitor-resistant virus from CXCR4-using HIV-1 without changing the V3 loop. The configuration of the V3 loop might be the major determinant for selection of such resistant viruses, which may also determine how the virus evolves for resistance or the coreceptor switch. Further structure-based analyses are necessary to elucidate these molecular mechanisms.

## Acknowledgments

We are grateful to Ms. Yoshiko Tamura for preparing the cDNAs of the viral RNA from CRF01_AE-infected individuals. We also thank Dr. Keiichi Tamamura at Tokyo Medical and Dental University for kindly providing T134, Drs. Kazuhisa Yoshimura and Yuzhe Yuan for helpful discussions, and Ms. Rina Kawano for technical assistance.

## Author Contributions

Conceived and designed the experiments: YM HT. Performed the experiments: HT YM. Analyzed the data: YM HT. Contributed reagents/materials/analysis tools: YN KM MT SO KY. Wrote the paper: YM SH.

## References

1. Symons J, van Lelyveld SF, Hoepelman AI, van Ham PM, de Jong D, et al. (2011) Maraviroc is able to inhibit dual-R5 viruses in a dual/mixed HIV-1-infected patient. J Antimicrob Chem 66: 890–895.
2. Toma J, Whitcomb JM, Petropoulos CJ, Huang W (2010) Dual-tropic HIV type 1 isolates vary dramatically in their utilization of CCR5 and CXCR4 coreceptors. AIDS 24: 2181–2186.
3. Hoffman TL, Doms RW (1999) HIV-1 envelope determinants for cell tropism and chemokine receptor use. Mol Memb Biol 16: 57–65.
4. Huang CC, Lam SN, Acharya P, Tang M, Xiang SH, et al. (2007) Structures of the CCR5 N terminus and of a tyrosine-sulfated antibody with HIV-1 gp120 and CD4. Science 317: 1930–1934.
5. Huang W, Eshleman SH, Toma J, Fransen S, Stawiski E, et al. (2007) Coreceptor tropism in human immunodeficiency virus type 1 subtype D: High prevalence of CXCR4 tropism and heterogeneous composition of viral populations. J Virol 81: 7885–7893.
6. Resch W, Hoffman N, Swanstrom R (2001) Improved success of phenotype prediction of the human immunodeficiency virus type 1 from envelope variable loop 3 sequence using neural networks. Virology 288: 51–62.
7. Ogert RA, Lee MK, Ross W, Buckler-White A, Martin MA, et al. (2001) N-linked glycosylation sites adjacent to and within the V1/V2 and the V3 loops of dualtropic human immunodeficiency virus type 1 isolate DH12 gp120 affect coreceptor usage and cellular tropism. J Virol 75: 5998–6006.
8. Pollakis G, Kang S, Kliphuis A, Chalaby MIM, Goudsmit J, et al. (2001) N-Linked glycosylation of the HIV type-1 gp120 envelope glycoprotein as a major determinant of CCR5 and CXCR4 coreceptor utilization. J Biol Chem 276: 13433–13441.
9. Polzer S, Dittmar MT, Schmitz H, Meyer B, Müller H, et al. (2001) Loss of N-linked glycans in the V3-loop region of gp120 is correlated to an enhanced infectivity of HIV-1. Glycobiology 11: 11–19.
10. Casper C, Naver L, Clevestig P, Belfrage E, Leitner T, et al. (2002) Coreceptor change appears after immune deficiency is established in children infected with different HIV-1 subtypes. AIDS Res Hum Retroviruses 18: 343–352.
11. Connor RI, Sheridan KE, Ceradini D, Choe S, Landau NR (1997) Change in coreceptor use correlates with disease progression in HIV-1-infected individuals. J Exp Med 185: 621–628.
12. Scarlatti G, Tresoldi E, Bjorndal A, Fredriksson R, Colognesi C, et al. (1997) In vivo evolution of HIV-1 co-receptor usage and sensitivity to chemokine-mediated suppression. Nat Med 3: 1259–1265.
13. Maeda Y, Foda M, Matsushita S, Harada S (2000) Involvement of both the V2 and V3 regions of the CCR5-tropic human immunodeficiency virus type 1 envelope in reduced sensitivity to macrophage inflammatory protein 1α. J Virol 74: 1787–1793.
14. Kuhmann S, Pugach P, Kunstman K (2004) Genetic and phenotypic analyses of human immunodeficiency virus type 1 escape from a small-molecule CCR5 inhibitor. J Virol 78: 2790–2807.
15. Marozsan AJ, Kuhmann SE, Morgan T, Herrera C, Rivera-Troche E, et al. (2005) Generation and properties of a human immunodeficiency virus type 1 isolate resistant to the small molecule CCR5 inhibitor, SCH-417690 (SCH-D). Virology 338: 182–199.
16. Pugach P, Marozsan AJ, Ketas TJ, Landes EL, Moore JP, et al. (2007) HIV-1 clones resistant to a small molecule CCR5 inhibitor use the inhibitor-bound form of CCR5 for entry. Virology 361: 212–228.
17. Trkola A, Kuhmann SE, Strizki JM, Maxwell E, Ketas T, et al. (2002) HIV-1 escape from a small molecule, CCR5-specific entry inhibitor does not involve CXCR4 use. Proc Nat Acad Sci USA 99: 395–400.
18. Westby M, Smith-Burchnell C, Mori J, Lewis M, Mosley M, et al. (2007) Reduced maximal inhibition in phenotypic susceptibility assays indicates that viral strains resistant to the CCR5 antagonist maraviroc utilize inhibitor-bound receptor for entry. J Virol 81: 2359–2371.
19. Yuan Y, Maeda Y, Terasawa H, Monde K, Harada S, et al. (2011) A combination of polymorphic mutations in V3 loop of HIV-1 gp120 can confer noncompetitive resistance to maraviroc. Virology 413: 293–299.
20. Yuan Y, Yokoyama M, Maeda Y, Terasawa H, Harada S, et al. (2013) Structure and dynamics of the gp120 V3 loop that confers noncompetitive resistance in R5 HIV-$1_{JR-FL}$ to maraviroc. PloS One 8: e65115.
21. Yusa K, Maeda Y, Fujioka A, Monde K, Harada S (2005) Isolation of TAK-779-resistant HIV-1 from an R5 HIV-1 GP120 V3 loop library. J Biol Chem 280: 30083–30090.
22. Este JA, Cabrera C, Blanco J, Gutierrez A, Bridger G, et al. (1999) Shift of clinical human immunodeficiency virus type 1 isolates from X4 to R5 and prevention of emergence of the syncytium-inducing phenotype by blockade of CXCR4. J Virol 73: 5577–5585.
23. Delobel P, Raymond S, Mavigner M, Cazabat M, Alvarez M, et al. (2010) Shift in phenotypic susceptibility suggests a competition mechanism in a case of acquired resistance to maraviroc. AIDS 24: 1382–1384.
24. Arakaki R, Tamamura H, Premanathan M, Kanbara K, Ramanan S, et al. (1999) T134, a small-molecule CXCR4 inhibitor, has no cross-drug resistance with AMD3100, a CXCR4 antagonist with a different structure. J Virol 73: 1719–1723.
25. Armand-Ugon M, Quinones-Mateu ME, Gutierez A, Barretina J, Blanco J, et al. (2003) Reduced fitness of HIV-1 resistant to CXCR4 antagonists. Antivir Ther 8: 1–8.
26. de Vreese K, Kofler-Mongold V, Leutgeb C, Weber V, Vermeire K, et al. (1996) The molecular target of bicyclams, potent inhibitors of human immunodeficiency virus replication. J Virol 70: 689–696.
27. Kanbara K, Sato S, Tanuma J, Tamamura H, Gotoh K, et al. (2001) Biological and genetic characterization of a human immunodeficiency virus strain resistant to CXCR4 antagonist T134. AIDS Res Hum Retroviruses 17: 615–622.
28. Moncunill G, Armand-Ugón M, Clotet-Codina I, Pauls E, Ballana E, et al. (2008) Anti-HIV activity and resistance profile of the CXC chemokine receptor 4 antagonist POL3026. Mol Pharm 73: 1264–1273.
29. Schols D, Struyf S, Van Damme J, Este JA, Henson G, et al. (1997) Inhibition of T-tropic HIV strains by selective antagonization of the chemokine receptor CXCR4. J Exp Med 186: 1383–1388.
30. Maeda Y, Yusa K, Harada S (2008) Altered sensitivity of an R5X4 HIV-1 strain 89.6 to coreceptor inhibitors by a single amino acid substitution in the V3 region of gp120. Antiviral Res 77: 128–135.
31. Schols D, Este JA, Henson G, De Clercq E (1997) Bicyclams, a class of potent anti-HIV agents, are targeted at the HIV coreceptor fusin/CXCR-4. Antiviral Res 35: 147–156.
32. Dorr P, Westby M, Dobbs S, Griffin P, Irvine B, et al. (2005) Maraviroc (UK-427, 857), a potent, orally bioavailable, and selective small-molecule inhibitor of chemokine receptor CCR5 with broad-spectrum anti-human immunodeficiency virus type 1 activity. Antimicrob Agents Chem 49: 4721–4732.
33. Platt EJ, Wehrly K, Kuhmann SE, Chesebro B, Kabat D (1998) Effects of CCR5 and CD4 cell surface concentrations on infections by macrophagetropic isolates of human immunodeficiency virus type 1. J Virol 72: 2855–2864.
34. Soda Y, Shimizu N, Jinno A, Liu HY, Kanbe K et al. (1999) Establishment of a new system for determination of coreceptor usages of HIV based on the human glioma NP-2 cell line. Biochem Biophys Res Commun 258: 313–321
35. Jinno A, Shimizu N, Soda Y, Haraguchi Y, Kitamura T, et al. (1998) Identification of the chemokine receptor TER1/CCR8 expressed in brain-derived cells and T cells as a new coreceptor for HIV-1 infection. Biochem Biophys Res Comm 243: 497–502.
36. Watanabe K, Murakoshi H, Tamura Y, Koyanagi M, Chikata T, et al. (2013) Identification of cross-clade CTL epitopes in HIV-1 clade A/E-infected individuals by using the clade B overlapping peptides. Microbes Infect 15: 874–886.

37. Pauwels R, Balzarini J, Baba M, Snoeck R, Schols D, et al. (1988) Rapid and automated tetrazolium-based colorimetric assay for the detection of anti-HIV compounds. J Virol Methods 20: 309–321.
38. Pramanik L, Fried U, Clevestig P, Ehrnst A (2011) Charged amino acid patterns of coreceptor use in the major subtypes of human immunodeficiency virus type 1. J Gen Virol 92: 1917–1922.
39. Lengauer T, Sander O, Sierra S, Thielen A, Kaiser R (2007) Bioinformatics prediction of HIV coreceptor usage. Nature biotechnology 25: 1407–1410.
40. Li Y, O'Dell S, Walker LM, Wu X, Guenaga J, et al. (2011) Mechanism of neutralization by the broadly neutralizing HIV-1 monoclonal antibody VRC01. J Virol 85: 8954–8967.
41. Fouchier RA, Groenink M, Kootstra NA, Tersmette M, Huisman HG, et al. (1992) Phenotype-associated sequence variation in the third variable domain of the human immunodeficiency virus type 1 gp120 molecule. J Virol 66: 3183–3187.
42. Shioda T, Levy JA, Cheng-Mayer C (1992) Small amino acid changes in the V3 hypervariable region of gp120 can affect the T-cell-line and macrophage tropism of human immunodeficiency virus type 1. Proc Nat Acad Sci USA 89: 9434–9438.
43. Kwong PD, Wyatt R, Robinson J, Sweet RW, Sodroski J, et al. (1998) Structure of an HIV gp120 envelope glycoprotein in complex with the CD4 receptor and a neutralizing human antibody. Nature 393: 648–659.
44. Rizzuto CD, Wyatt R, Hernandez-Ramos N, Sun Y, Kwong PD, et al. (1998) A conserved HIV gp120 glycoprotein structure involved in chemokine receptor binding. Science 280: 1949–1953.
45. Wyatt R, Kwong PD, Desjardins E, Sweet RW, Robinson J, et al. (1998) The antigenic structure of the HIV gp120 envelope glycoprotein. Nature 393: 705–711.
46. Harrison JE, Lynch JB, Sierra L-J, Blackburn LA, Ray N, et al. (2008) Baseline resistance of primary human immunodeficiency virus type 1 strains to the CXCR4 inhibitor AMD3100. J Virol 82: 11695–11704.
47. Reeves JD, Miamidian JL, Biscone MJ, Lee F-H, Ahmad N, et al. (2004) Impact of mutations in the coreceptor binding site on human immunodeficiency virus type 1 fusion, infection, and entry inhibitor sensitivity. J Virol 78: 5476–5485.
48. Suphaphiphat P, Essex M, Lee TH (2007) Mutations in the V3 stem versus the V3 crown and C4 region have different effects on the binding and fusion steps of human immunodeficiency virus type 1 gp120 interaction with the CCR5 coreceptor. Virology 360: 182–190.
49. Suphaphiphat P, Thitithanyanont A, Paca-Uccaralertkun S, Essex M, Lee TH (2003) Effect of amino acid substitution of the V3 and bridging sheet residues in human immunodeficiency virus type 1 subtype C gp120 on CCR5 utilization. J Virol 77: 3832–3837.
50. Anastassopoulou CG, Marozsan AJ, Matet A, Snyder AD, Arts EJ, et al. (2007) Escape of HIV-1 from a small molecule CCR5 inhibitor is not associated with a fitness loss. PLoS pathog 3: e79.
51. Anastassopoulou CG, Ketas TJ, Klasse PJ, Moore JP (2009) Resistance to CCR5 inhibitors caused by sequence changes in the fusion peptide of HIV-1 gp41. Proc Nat Acad Sci USA 106: 5318–5323.
52. Zhou T, Georgiev I, Wu X, Yang ZY, Dai K, et al. (2010) Structural basis for broad and potent neutralization of HIV-1 by antibody VRC01. Science 329: 811–817.
53. Hatse S, Princen K, Gerlach LO, Bridger G, Henson G, et al. (2001) Mutation of Asp(171) and Asp(262) of the chemokine receptor CXCR4 impairs its coreceptor function for human immunodeficiency virus-1 entry and abrogates the antagonistic activity of AMD3100. Mol Pharm 60: 164–173.
54. Labrosse B, Brelot A, Heveker N, Sol N, Schols D, et al. (1998) Determinants for sensitivity of human immunodeficiency virus coreceptor CXCR4 to the bicyclam AMD3100. J Virol 72: 6381–6388.
55. Kajumo F, Thompson DA, Guo Y, Dragic T (2000) Entry of R5X4 and X4 human immunodeficiency virus type 1 strains is mediated by negatively charged and tyrosine residues in the amino-terminal domain and the second extracellular loop of CXCR4. Virology 271: 240–247.

Kasahara et al. Virology Journal 2013, 10:338
http://www.virologyj.com/content/10/1/338

VIROLOGY JOURNAL

RESEARCH Open Access

# Natural OX40L expressed on human T cell leukemia virus type-I-immortalized T cell lines interferes with infection of activated peripheral blood mononuclear cells by CCR5-utilizing human immunodeficiency virus

Daigo Kasahara[1], Azusa Takara[1], Yoshiaki Takahashi[1], Akira Kodama[1], Reiko Tanaka[1], Aftab A Ansari[2] and Yuetsu Tanaka[1*]

## Abstract

**Background:** OX40 ligand (OX40L) co-stimulates and differentiates T cells via ligation of OX40 that is transiently induced on T cells upon activation, resulting in prolonged T cell survival and enhanced cytokine production by T cells. This view has led to the targeting of OX40 as a strategy to boost antigen specific T cells in the context of vaccination. In addition, the ligation of OX40 has also been shown to inhibit infection by CCR5-utilizing (R5) but not CXCR4-utilizing (X4) human immunodeficiency virus type-1 (HIV-1) via enhancement of production of CCR5-binding β-chemokines. It was reasoned that human T cell leukemia virus type-I (HTLV-1) immortalized T cell lines that express high levels of OX40L could serve as an unique source of physiologically functional OX40L. The fact that HTLV-1$^+$ T cell lines simultaneously also express high levels of OX40 suggested a potential limitation.

**Results:** Results of our studies showed that HTLV-1$^+$ T cell lines bound exogenous OX40 but not OX40L, indicating that HTLV-1$^+$ T cell lines express an active form of OX40L but an inactive form of OX40. Anti-OX40 non-blocking monoclonal antibody (mAb), but not blocking mAb, stained HTLV-1$^+$ T cell lines, suggesting that the OX40 might be saturated with endogenous OX40L. Functionality of the OX40L was confirmed by the fact that a paraformaldehyde (PFA)-fixed HTLV-1$^+$ T cell lines inhibited the infection of autologous activated peripheral blood mononuclear cells (PBMCs) with R5 HIV-1 which was reversed by either anti-OX40L blocking mAb or a mixture of neutralizing mAbs against CCR5-binding β-chemokines.

**Conclusions:** Altogether, these results demonstrated that autologous T cell lines immortalized by HTLV-1 can be utilized as a conventional source of physiologically functional OX40L.

## Background

OX40 ligand (OX40L, CD252) belonging to the tumor necrosis factor (TNF) superfamily is a co-stimulatory molecule [1,2] that was first described by our laboratory as gp34 that is constitutively expressed at high levels on the surface of human T cell leukemia virus type-I (HTLV-1)-immortalized T cell lines [3,4]. It is now clear that OX40L can be induced on a wide variety of human hematopoietic cell lineages including antigen presenting cells (APCs) such as dendritic cells (DCs) [5] and B cells [6], natural killer (NK) cells [7], mast cells [8], endothelial cells [9] and T cells [10,11]. OX40 (CD134), a member of the TNF receptor (TNFR) superfamily that is rapidly induced predominantly on T cells upon cell activation is the cognate receptor for OX40L [12-14]. Interaction of OX40 on T cells with OX40L on APCs generates a variety of biological changes that include enhanced production of cytokines by T cells, Th2 cell differentiation, prolonged T cell survival, activation of B cells and DCs, to name a few

* Correspondence: yuetsu@s4.dion.ne.jp
[1]Department of Immunology, Graduate School of Medicine, University of the Ryukyus, Okinawa 903-0215, Japan
Full list of author information is available at the end of the article

[1,12,15]. OX40L is naturally expressed on the cell surface as a trimeric protein that binds to three copies of monomeric OX40 within close proximity [16]. Such close interactions between OX40/OX40L promotes tight cell to cell adhesion facilitating T cell-DC communication and skin infiltration of $OX40^+$ leukemic T cells in adult T cell leukemia (ATL) [17].

It has been proposed that the targeting of OX40 on activated T cells by OX40L or with the use of anti-OX40 agonistic antibodies may provide a strategy for the selective expansion of the limited frequencies of antigen specific T cells that are normally induced during vaccination and thereby achieve more effective immune responses [18-20]. Another immunological role of OX40L-OX40 interaction that we have previously documented includes the ability of OX40L in either soluble or membrane-bound form to effectively inhibit the infection of activated PBMCs with R5 HIV-1 *in vitro* [21]. This inhibition was shown to be mediated via the enhanced production of the CCR5-binding β-chemokines that include RANTES, MIP-1α and MIP-1β, followed by the down-modulation of cell surface CCR5 expression. These findings brought into focus the potential use of OX40L as a therapeutic tool and prompted us to investigate methodologies that would provide a convenient source for biologically active OX40L. One such source of OX40L was reasoned to be $HTLV\text{-}1^+$ T cell lines that unlike normal activated T cells or non-T cells have been shown to express both OX40L and OX40 on the cell surface at a single cell level due to the action of the HTLV-1-encoded oncogenic protein Tax [4,22]. Tax, in addition, also induces the expression of 4-1BB and its cognate ligand both of which belong to the TNF/TNFR family [23]. Selective induction of these ligand/receptor pairs has been implicated in the survival of HTLV-1-infected cells.

Studies were therefore carried out in efforts to examine whether OX40L and OX40 were expressed in a biologically active form by $HTLV\text{-}1^+$ T cell lines. We report herein for the first time that $HTLV\text{-}1^+$ T cell lines express a biologically active form of OX40L while the OX40 molecule appears biologically inactive or masked. The OX40L expressed by $HTLV\text{-}1^+$ T cell lines was capable of inhibiting R5 HIV-1 infection of activated PBMCs via production of CCR5-binding β-chemokines. These findings suggest that autologous HTLV-1-immortalized T cell lines can be utilized as a readily available convenient source of natural OX40L in large quantities for various immunological studies.

## Results

### HTLV-1-immortalized T cell lines express active OX40L together with inactive OX40

In order to determine whether OX40L and OX40 co-expressed on the cell surface of $HTLV\text{-}1^+$ T cell lines were biologically active, we examined their capacities to bind biotinylated rec-OX40 and rec-OX40L, respectively. The finding that rec-OX40 and rec-OX40L bound specifically to the OX40L-transfected CEM cells (CEM/OX40L) and the OX40-transfected CEM/OX40 cells, respectively, demonstrated the specificity of the assay being utilized (Figure 1). Interestingly, although the standard $HTLV\text{-}1^+$ T cell line (MT-2) was stained double positive with anti-OX40L (clone 5A8) and anti-OX40 (clone B-7B5) mAbs, they bound only rec-OX40 but not rec-OX40L. This finding indicated that while OX40L was expressed in an active form on MT-2 cells, the OX40 was likely to be expressed in an inactive form. Similar results were obtained by the testing of a number of additional $HTLV\text{-}1^+$ T cell lines, including T cell lines spontaneously established from a HTLV-1-infected patient with adult T cell leukemia (ILT-H2) and a HTLV-1-associated myelopathy (HAM/TSP) patient (ILT-M1), and various *in vitro*-HTLV-1-immortalized $CD4^+$ or $CD8^+$ T cell lines from different healthy donors (such as YT/cM1, RT/cH2 cells) (Figure 1). Thus, these results suggest that on the cell surface of the $HTLV\text{-}1^+$ T cell lines only OX40L, but not OX40, is capable of binding its respective ligand.

### Characterization of OX40 on $HTLV\text{-}1^+$ T cells

A series of studies were subsequently conducted in efforts to identify the potential reason(s) for the failure of $HTLV\text{-}1^+$ T cell lines to bind rec-OX40L. Western Blot analysis of OX40 expressed by $HTLV\text{-}1^+$ T cell line was first carried out to determine whether the OX40 expressed by these cells was truncated. Cell lysates prepared from surface biotinylated *in vitro* activated PBMCs and the OX40 transfected CEM cell line (CEM/OX40) were analyzed in parallel with the $HTLV\text{-}1^+$ T cell line MT-2 using standard Western Blot techniques. Results of these studies displayed in Figure 2 showed that there were no detectable differences in the molecular weight of the glycosylated authentic OX40 (50 kDa) among these three samples. The 35 kDa band corresponding to the non-glycosylated form of OX40 was apparent in CEM/OX40 cells and activated PBMCs, but it was faint in MT-2 cells. These data indicated that there was no detectable deletion or modification in the glycosylated OX40 molecules expressed by the $HTLV\text{-}1^+$ T cell lines.

To further probe for the molecular basis for the inability of the OX40 expressed by the $HTLV\text{-}1^+$ T cell lines to bind rec-OX40L, we utilized an additional anti-OX40 specific mAb (W4-54 mAb) along with B-7B5 mAb. While the clone W4-54 anti-OX40 mAb inhibited the binding of OX40 and OX40L, the clone B-7B5 failed to show any detectable inhibition (Additional file 1: Figure S1). These two mAbs are reasoned to react against conformational epitopes since they failed to bind any overlapping 15-mer peptides spanning the entire OX40 protein (data not shown). As shown in Figure 3(A), control mock treated CEM/

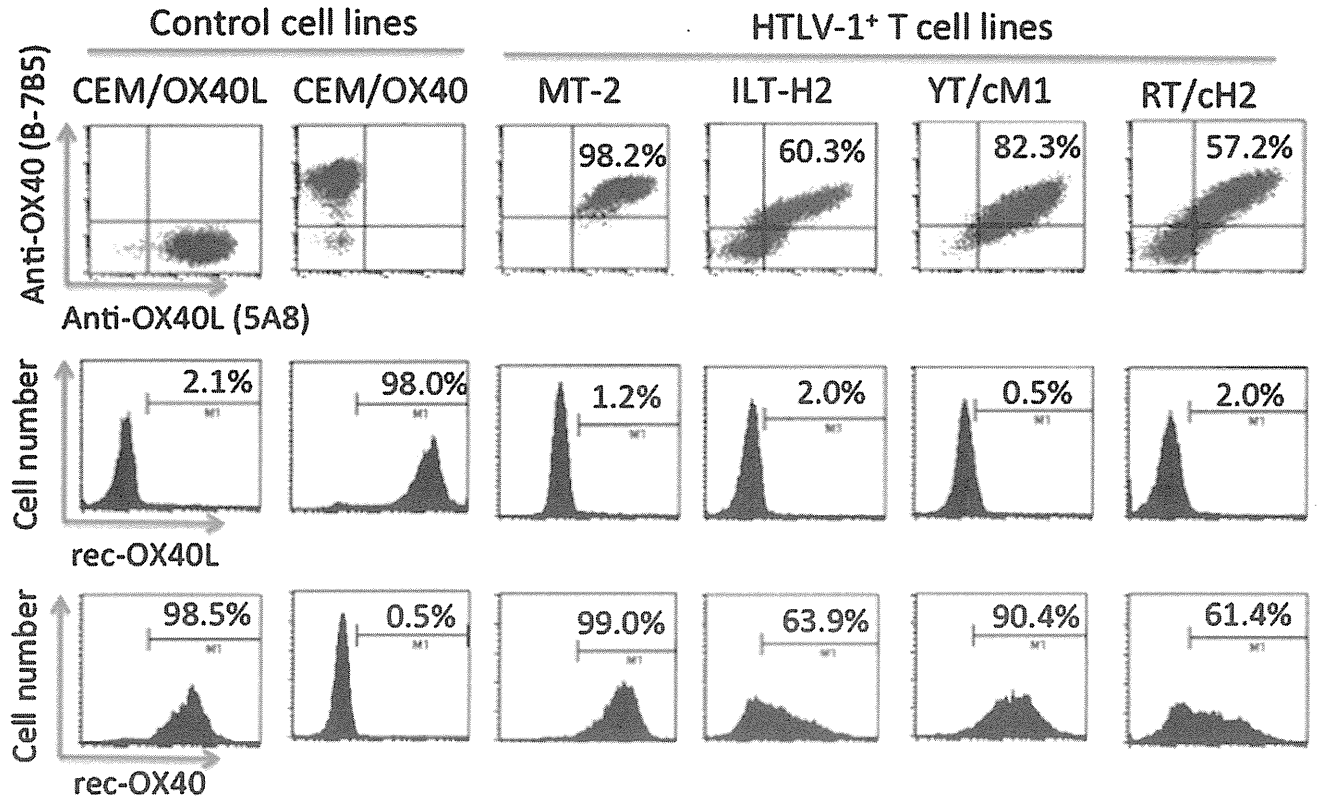


**Figure 1 HTLV-1$^+$ T cells co-express both OX40L and OX40 but only OX40L is expressed in an active form.** The OX40 and OX40L co-expressing control CEM cells and the HTLV-1$^+$ cells were dually stained with FITC-labeled anti-OX40 (B-7B5) and Cy-5 labeled anti-OX40L (5A8) (upper row), or singly stained either with biotinylated recombinant OX40L (rec-OX40L) or rec-OX40 followed by PE-streptavidin (middle and lower rows, respectively). Data shown are representative profiles of 3 independent experiments.

OX40 and activated PBMCs, as expected, both stained dual-positive with the B-7B5 mAb and W4-54 mAbs. These data show that the comparative staining with B-7B5 and W4-54 mAbs can be potentially utilized to distinguish between non-ligated versus OX40L ligated forms of OX40. Figure 3(B) shows that although B-7B5 mAb stained HTLV-1$^+$ T cell lines at high levels, little or no staining was noted with the use of the W4-54 mAb. In contrast, results of a WB analysis showed that the W4-54 mAb readily reacts to the p50 of the OX40 molecule in lysates of the HTLV-1$^+$ T cell line, YT/cM1 (Additional file 2: Figure S2). These results suggest that the OX40L binding site of OX40 expressed by the HTLV-1$^+$ T cell lines was altered, most probably due to pre-occupation with endogenous OX40L. To confirm this possibility, we explored the presence of OX40-OX40L complexes expressed by HTLV-1$^+$ T cell lines using our in-house ELISA. Cell lysates of the ATL-derived HTLV-1$^+$ T cell line (ILT-H2) were first captured with the use of immobilized anti-OX40L (clone HD-1) or anti-OX40 (clone B-7B5) mAb, respectively. The levels of captured antigens were assayed with the use of HRP-labeled anti-OX40 mAb or anti-OX40L mAb. Although it is reasonable to assume that the natural interaction between OX40 and OX40L on the living cell surface may be dissociated by the detergent treatment, as shown in Figure 4, low but significant levels of OX40-OX40L complex were still detectable in the cell lysates.

### Functional OX40L expressed by HTLV-1$^+$ T cell lines

To confirm that the OX40L expressed on the HTLV-1$^+$ T cell lines is biologically functional, we performed co-culture experiments using the experimental *in vitro* infection of autologous activated PBMCs with HIV-1 as a read out. PBMCs activated with anti-CD3/anti-CD28 mAbs for 24 hours were washed and infected with either R5 HIV-$1_{JR\text{-}FL}$ or X4 HIV-$1_{NL4\text{-}3}$ at a low m.o.i., and then co-cultured with paraformaldehyde (PFA)-fixed autologous HTLV-1$^+$ T cell line in the presence or absence of anti-OX40L mAb or a mixture of the three CCR5-binding chemokine-blocking mAbs (anti-RANTES, anti-MIP-1α and anti-MIP-1β). The reasons why we utilized autologous PFA-fixed HTLV-1$^+$ T cell lines were to avoid any allogeneic stimuli and minimize the secretion of any anti-HIV-1 factors by the HTLV-1$^+$ T cell lines. As shown in Figure 5, the frequencies of HIV-1 p24$^+$ T cells in the cultures were reduced by co-culture with not only autologous HTLV-1$^+$ T cell line but also with the

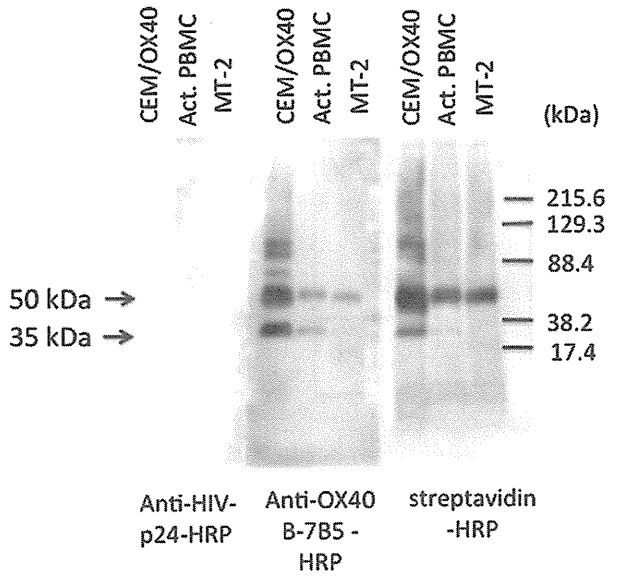


**Figure 2 Western blot analysis of OX40.** OX40-expressing CEM cells (CEM/OX40), *in vitro* activated PBMCs and MT-2 cells were cell-surface labeled with biotin, lysed and immunoprecipitated with anti-OX40 (B-7B5). The precipitates were subjected to 10% PAGE and blotted onto nitrocellulose sheets. The sheets were then probed with HRP-labeled anti-HIV-1 p24 (as a control), anti-OX40 (B-7B5) or streptavidin. Mol. Wt. markers are shown on the right. Data shown are representative of 3 independent experiments.

addition of soluble rec-OX40L. This inhibition was mediated by OX40L-OX40 interaction since the addition of the anti-OX40L blocking mAb (clone 5A8) and/or the addition of a mixture of the anti-β-chemokine mAbs reversed the level of reduction. It is worthy to note that, similar to data we have previously reported with the use of recombinant OX40L [21], X4 HIV-1 infection was not influenced by co-cultivation with PFA-fixed HTLV-1$^+$ T cell line, suggesting the CCR5-specificity of this antiviral effect.

Finally, we compared the potential of membrane bound OX40L of the fixed HTLV-1$^+$ T cell lines with that of soluble rec-OX40L to inhibit R5 HIV-1 infection by the quantitation of p24 production in the culture supernatants. As shown in Figure 6, whereas the inhibitory effect of the rec-OX40L reached a plateau at levels > 1.25 μg/ml, the autologous HTLV-1$^+$ T cell line could inhibit more effectively at even an HTLV-1$^+$ T cell to PBMCs ratio as low as 0.3. The maximum inhibition reached with rec-OX40 was around 65% of the maximum inhibition reached with HTLV-1$^+$ T cell line, with similar $IC_{50}$. Altogether, these data demonstrate that indeed, the OX40L expressed by HTLV-1$^+$ T cell lines is biologically active.

## Discussion

In the present study, we revealed that the cell surface expressed OX40L on T cell lines immortalized by HTLV-1 is biologically active in concert with the co-expression of an inactive form of OX40. As far as we know, this is the first study to report the polarized "OX40L-active/OX40 inactive" expression by HTLV-1$^+$ T cell lines. The expression of active forms of OX40L is not unique to HTLV-1$^+$ T cell lines, since similar conditions have also been observed in normal T cells when they are activated under mild DNA damaging conditions or cultured for long-term in IL-2 containing media with periodic stimulation [11,24]. However, compared to these normal T cells, HTLV-1$^+$ T cell lines are immortal and thus can provide unlimited amounts of OX40L.

The precise mechanism for the inability of OX40 on HTLV-1$^+$ T cell lines to bind OX40L remains to be clearly defined. Based on our previous paper showing that functional OX40L can be transferred to OX40 intercellularly [25], we hypothesize that the cell surface OX40 may be saturated with endogenously produced OX40L in *cis* and/or *trans* mode. Indeed, the WB analysis showed that the OX40-OX40L blocking mAb W4-54 that did not stain living HTLV-1$^+$ T cells reacted to the p50 OX40 molecule (Additional file 2: Figures S2 and Additional file 3: Figures S3). In accordance with this assumption, we demonstrated the presence of OX40-OX40L complexes in lysates of HTLV-1$^+$ T cell lines by ELISA (Figure 4). It remains unclear why there were significant amounts of OX40L-free OX40 molecules in the lysates from HTLV-1$^+$ T cells as determined by ELISA. It will be highly likely that the detergent treatment dissociates the OX40 and OX40L complex due to perturbation of cytoplasmic membrane structure including lipid rafts on which OX40 is supposed to reside in association with the other TNFR member such as 4-1BB [26,27]. In addition, our preliminary data that supports the OX40 saturation hypothesis includes the finding using the HUT 102 cell line that is another HTLV-1$^+$ T cell line from which the original OX40 gene was cloned [13]. This HUT102 cell line stained with both B-7B5 and W4-54 mAbs, but not with anti-OX40L (5A8 mAb), and was able to bind recombinant OX40L but not OX40 (Additional file 3: Figure S3). Although it is not clear why HUT102 cell line was positive for Tax antigen but negative for OX40L expression, these data clearly showed that in the absence of OX40L, functional OX40 can be expressed on the cell surface. It will be of interest to examine whether the inactive form of the OX40 can be converted to an active form after silencing the expression of OX40L in HTLV-1$^+$ T cell lines. Such studies are currently in progress.

On the basis of the present and previous results on OX40L [21], it can be hypothesized that OX40L may have a therapeutic and prophylactic potential against R5 HIV-1 infection. However, at present, purified biologically active forms of human OX40L protein in large quantities is not available. The alternative is to utilize

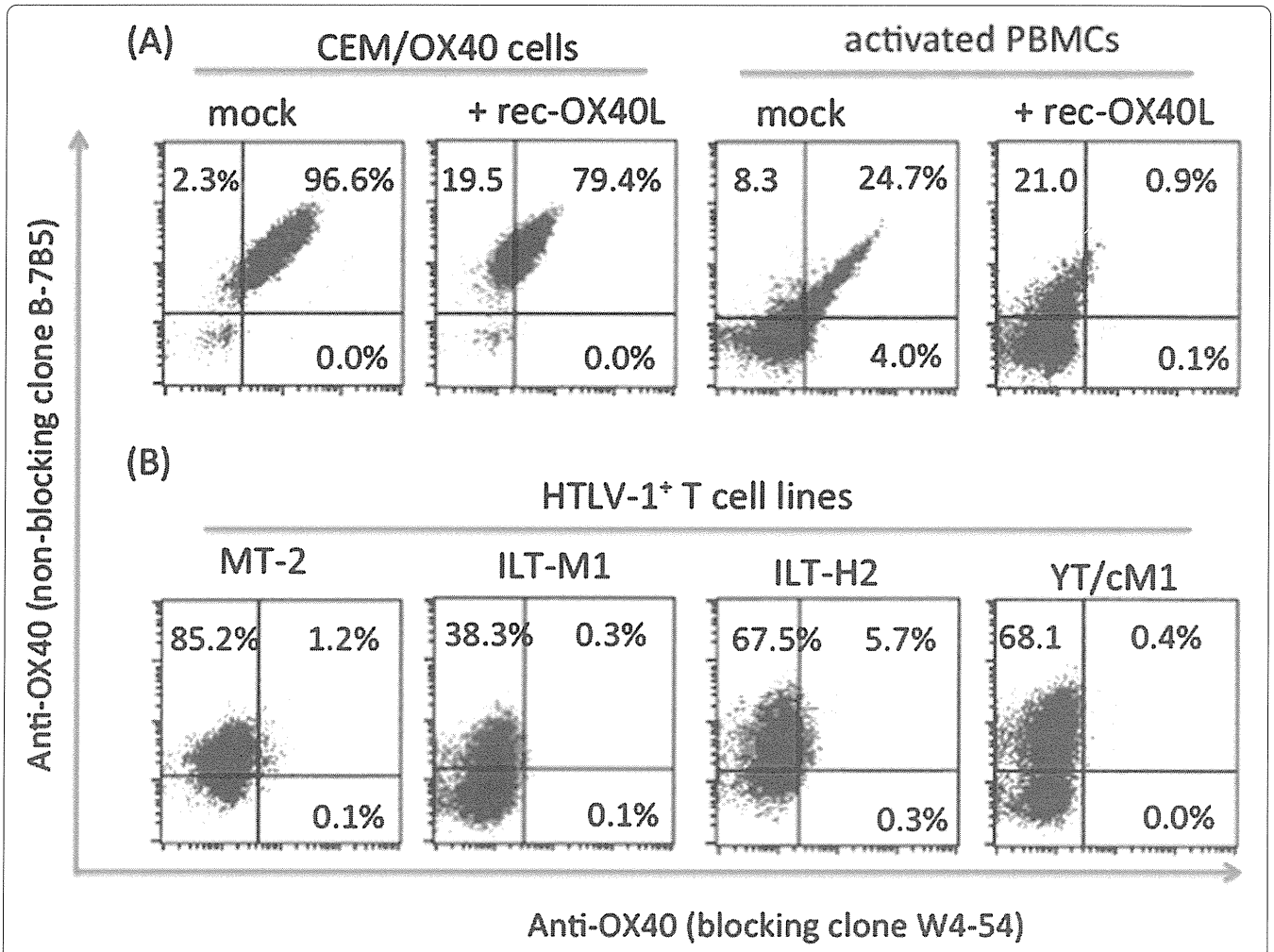


**Figure 3 Blocking (clone W4-54) versus non-blocking (clone B-7B5) mAb against 2 distinct epitopes of OX40 distinguish between OX40L bound and unbound OX40. (A)** OX40-expressing CEM and activated PBMCs were stained with the two mAbs in the absence (mock) or presence of 1 μg/ml of recombinant OX40L (rec-OX40L). **(B)** Various HTLV-1$^+$ T cell lines were stained with B-7B5 andW4-54 labeled with FITC and Cy5, respectively. Data shown are representative of 3 independent experiments.

OX40L-fusion proteins [28], OX40L-expressing recombinant virus [20], OX40L mRNA-transfected cells [29], lentivirus-transduced DCs [30], or autologous dying normal T cells [24]. The superiority of using cell membrane-bound OX40L as compared with the use of a soluble form was documented by data observed by the degree of inhibition of R5 HIV-1 as seen in the present study (Figure 6). These findings are in accord with a previous study that showed that the membrane-immobilized form of OX40L is highly active in the stimulation of an OX40-transfected cell line to produce cytokines [31]. In addition to OX40L, HTLV-1$^+$ cell lines may exert additional suppressing effect on R5 HIV-1 infection via Tax protein, since Tax proteins of HTLV-1 and HTLV-2 have been shown to play a role in generating antiviral responses against HIV-1 via induction of CCR5-binding chemokines *in vitro* [32]. This view is supported by the finding that co-infection with HTLV interferes with the progression of HIV-1 disease *in vivo* [33]. However, such Tax effects in the present study may be less potent than OX40L since anti-OX40L mAb significantly reversed the suppression of R5-HIV-1 induced by co-culture with autologous HTLV-1$^+$ T cell lines (Figure 5).

## Conclusions

The present results demonstrate that HTLV-1$^+$ T cell line is a unique source of functional human OX40L, and suggest that autologous HTLV-1-immortalized T cell lines can be utilized as a conventional source of natural and functional OX40L in large quantities for various immunological studies.

## Methods

### Reagents

The medium used throughout the studies consisted of RPMI 1640 medium (Sigma-Aldrich. Inc. St. Louis, MO), supplemented with 10% fetal calf serum (FCS), 100 U/ml

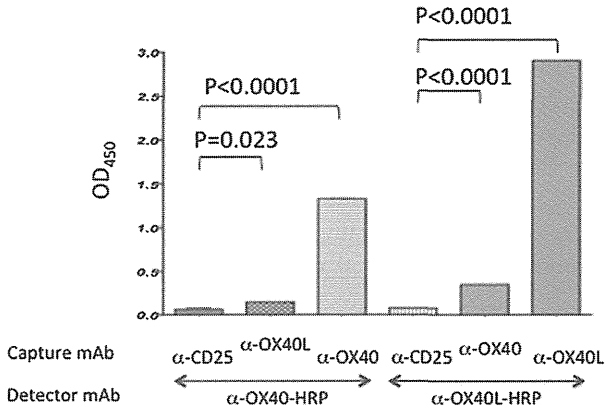


**Figure 4 Presence of OX40-OX40L complexes in HTLV-1$^+$ T cell lysates.** The ILT-H2 cell line derived from an ATL patient were lysed and the lysates incubated in microtiter wells that had been previously coated with either anti-CD25, OX40 or OX40L mAb for 1 hour. Anti-CD25 mAb was used as a non-specific negative control. After washing, the levels of OX40 or OX40L bound to the plates were assayed using either HRP-labeled anti-OX40 or anti-OX40L mAb. Data shown are representative of 3 independent experiments.

penicillin and 100 μg/ml streptomycin (hereinafter called RPMI medium). Anti-human CD3 mAb (clone OKT-3) and agonistic anti-CD28 mAb were purchased from the American Type Culture Collection (Rockville, MD) and Biolegend (San Diego, CA), respectively. Neutralizing mAbs against human RANTES, MIP-1α, and MIP-1β were purchased from R&D systems (Minneapolis, MN). The mouse mAbs produced in our laboratory included anti-OX40L (blocking clone 5A8 [34] and clone HD1, unpublished), anti-human OX40 (non-blocking clone B-7B5 and clone 17D8 [35]), anti-HIV-1 p24 (clones NP-24 and 2C2 [21]) and anti-CD25 (clone H-8) [36]. The rat mAbs included anti-human OX40 (blocking clone W4-54) and anti-HCV (clone Mo-8) [25,37]). Some clones were labeled with HRP using a kit (Dojin, Kumamoto, Japan) and used as the detector mAb in ELISA. These in-house mAbs were isolated from ascites fluid prepared in Balb/c or CB.17-SCID mice. The IgGs were purified utilizing a standard gel filtration method. Some of them were labeled with FITC, HiLyte Fluor 647 or Cy5 using commercial labeling kits (Dojin, GE Healthcare) according to the manufacturer's instructions. Biotinylated recombinant-soluble human OX40 (sOX40 in a form of murine IgG2a-Fc fusion protein) and OX40L (sOX40L in a form of murine CD8-fusion protein) were purchased from Ancell (Bayport, MN) and used with PE-streptavidin (BioLegend) for staining. Unlabeled glycosylated recombinant human OX40L that consists of OX40L with a human CD33 signal peptide produced in NS1 cells was purchased from R&D systems. Human recombinant IL-2 was obtained as a courtesy from the NIH-AIDS Reagent and Repository program (Bethesda, MD).

### Cell lines

The HTLV-1-producing T cell lines used included the MT-2, HUT102 and the IL-2 dependent T cell lines ILT-M1 and ILT-H2 that had been generated from a HTLV-1-associated myelopathy (HAM) and an adult T cell leukemia (ATL) patient, respectively. Additional cell lines utilized included the CEM cell lines transfected with either human OX40L or OX40 (CEM/OX40L and CEM/OX40) [38]. T cells isolated from normal human donors were immortalized by HTLV-1 as follows.

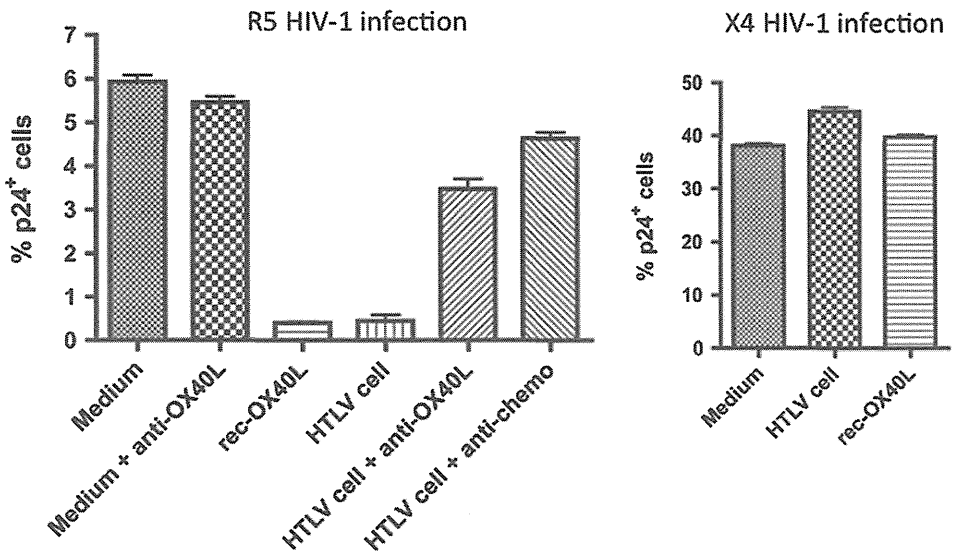


**Figure 5 PFA-inactivated HTLV-1$^+$ T cells inhibit infection of activated autologous PBMCs with R5 HIV-1, but not X4 HIV-1, via OX40L and β-chemokines.** In vitro activated PBMCs were infected with either R5 HIV-1 (JR-FL strain) or X4 HIV-1 (NL4-3 strain) and cultured in the presence or absence of recombinant OX40L, PFA-inactivated autologous HTLV-1$^+$ T cells, anti-OX40L blocking mAb (5A8) or a mixture of anti-β-chemokine neutralizing mAbs. After 4 days, the cells were examined for intracellular HIV-1 p24 by FCM. Data shown are representative of 3 independent experiments.

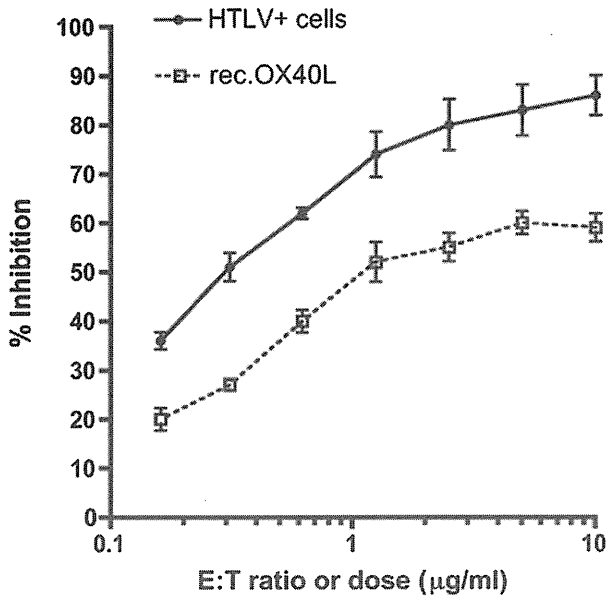


**Figure 6 HTLV-1$^+$ T cells are more potent in the inhibition of R5 HIV-1 infection than recombinant soluble OX40L.** R5 HIV-1-infected PBMCs prepared as in Figure 5 were cultured in the presence or absence of a graded concentration of recombinant soluble OX40L or PFA-fixed autologous HTLV-1$^+$ T cells. After 4 days, the levels of p24 produced in the culture supernatants were quantitated by ELISA. Data shown are representative of 2 independent experiments.

PBMCs from healthy donors were obtained by density gradient centrifugation of heparinized whole blood on HistoPAQUE-1077 (Sigma-Aldrich), suspended at 2 × $10^6$ cells/ml in RPMI medium, dispensed into individual wells of 24-well plates (BD) (1 ml/well) pre-coated with 5 μg/ml OKT3 for 1 hour and cultured in the presence of soluble 0.1 μg/ml anti-CD28 mAb. After 24 hours at 37°C in a 5% $CO_2$ humidified atmosphere, the activated PBMCs were harvested and washed once. These activated PBMCs (1 × $10^6$ cells/ml) were mixed with an equal number of ILT-M1 cells that were pretreated with 50 μg/ml MMC for 30 min at 37°C and cultured in RPMI media supplemented with 20 U/ml IL-2 (culture media). The cultures were performed in 24-well plates (BD) (2 ml/well) and the culture media was replenished every 3–4 days. After 1 ~ 2 months when HTLV-1 Tax$^+$ T cells appeared and started to grow continuously, they were split every 3 to 5 days using the culture medium.

### Flow Cytometry (FCM)

FCM analysis of live cells was carried out as described previously. Briefly, cells to be analyzed were Fc-blocked with 2 mg/ml normal human pooled IgG on ice for 15 min. Aliquots of these cells were then subjected to staining using pre-determined optimum concentrations of fluorescent dye-conjugated mAbs for 30 min on ice. The cells were then washed using FACS buffer (PBS containing 2% FCS and 0.1% sodium azide), fixed in 1% paraformaldehyde (PFA) containing FACS buffer and analyzed using a FACS Calibur, and the data obtained were analyzed using the Cell Quest software (BD). In order to determine whether cell surface OX40 or OX40L is functional, aliquots of Fc-blocked cells were incubated with either biotinylated recombinant-OX40L (rec-OX40L) or rec-OX40 at a concentration of 2.5 μg/ml for 30 minutes on ice, followed by staining with PE-labeled streptavidin (Beckman Coulter) for 30 minutes on ice and then analyzed by FCM. For detection of HIV-1 infected cells, PBMCs were fixed with PBS containing 4% PFA followed by washing twice in FACS buffer containing 0.5% saponin. These cells were Fc-blocked with 2 mg/ml normal human pooled IgG on ice for 15 min, and aliquots of these cells were stained with FITC- or Cy5-conjugated anti-HIV-1 p24 mAb (clone 2C2) for 30 min on ice. The cells were then washed using FACS buffer and absolute cell counts of p24$^+$ cells were performed by FCM using a cell counting kit (BD) according to the manufacturer's protocol. For staining of Tax antigen, cells were fixed with PBS containing 4% PFA followed by washing in FACS buffer containing 0.5% saponin. Aliquots of these cells were stained with Cy5-conjugated mouse anti-Tax mAb (Lt-4) [39] for 30 min on ice.

### ELISA and Western blot

For the quantitation of OX40L and OX40 by ELISA, anti-OX40L capture mAb (clone HD1)/ HRP-labeled detector mAb (clone 8F4) and anti-OX40 (clone B-7B5)/ HRP-labeled detector mAb (clone 17D8), respectively, were used together with recombinant standard proteins purchased from R&D systems. Immunoprecipitation followed by Western blot analysis of OX40 was performed as reported previously [40].

### HIV-1 preparation and infection

HIV-$1_{JR\text{-}FL}$ and HIV-$1_{NL4\text{-}3}$ viral stocks were produced as described previously [21]. *In vitro* activated PBMCs were prepared as described above, washed once and infected with either R5 HIV-$1_{JR\text{-}FL}$ or X4 HIV-$1_{NL4\text{-}3}$ at a multiplicity of infection (m.o.i.) of 0.005 for 2 hours. After washing 3 times, PBMCs were re-suspended at 1 × $10^6$ cells/ml in 20 U/ml IL-2-containing RPMI medium, dispensed into individual wells of 48-well plates (BD) (0.5 ml/well) and cultured in the presence or absence of 1 μg/ml of rec-OX40L or graded numbers of autologous HTLV-1$^+$ T cells (HTLV-1$^+$ T cells : PBMCs ratio of 10 to 0.15) that had been previously inactivated with 4% paraformaldehyde (PFA). Production of HIV-1 was determined by either the measurement of HIV-1 core p24 levels produced in the culture supernatants using our in-house formulated and standardized kits or FCM using Cy5 labeled anti-HIV-1 p24 mAb [21].

### Statistical analysis

Data were tested for significance using the Student's *t* test by using Prism software (GraphPad Software).

## Additional files

**Additional file 1: Figure S1.** Characterization of two anti-human OX40 mAbs. In the presence of B-7B5, W4-54 or isotype control mAbs, the OX40 and OX40L co-expressing control CEM cells were singly stained either with biotinylated recombinant OX40L (rec-OX40L) or rec-OX40, respectively, followed by PE-streptavidin. Data shown are representative profiles of 3 independent experiments.

**Additional file 2: Figure S2.** Detection of OX40 expressed by HTLV-1$^+$ T cell line (YT/cM1) by Western Blot with B-7B5 and W4-54 mAbs. Cell lysates of HTLV-1$^+$ T cell line, YT/cM1, were subjected to 10% PAGE and blotted onto nitrocellulose sheets. The sheets were then probed with anti-OX40 mAbs (B-7B5 or W4-54) or isotype controls followed by goat anti-mouse IgG or anti-rat IgG. Mol. Wt. markers are shown on the right. Data shown are representative of 2 independent experiments.

**Additional file 3: Figure S3.** Phenotype of HUT-102 cell line. Phenotype of HUT-102 cells were examined by FCM using anti-OX40 mAbs (FITC-labeled B-7B5 and Cy5-labeled W4-54), anti-OX40L (Cy5-labeled 5A8), biotinylated OX40 (rec-OX40) and OX40L (rec-OX40L) followed by PE-streptavidin. Intracellular Tax antigen was stained by mouse anti-Tax Lt-4 mAb.

### Competing interests

The authors declare no competing financial interests.

### Authors' contributions

DK and YTak generated HTLV-1$^+$ T cell lines and carried out the FCM and ELISA, performed the statistical analysis and drafted the manuscript. AT performed WB and FCM analyses. AK produced R5 and X4 HIV-1 and titrated. RT produced and labeled antibodies, confirmed their specificities and made in-house ELISA. AAA participated in the design of the study and helped to draft the manuscript. YT conceived of the study, participated in its design and coordination, carried out the HIV-1 infection experiments and drafted the manuscript. All authors read and approved the final manuscript.

### Acknowledgements

This work was supported by grants from a Grant-in-Aid from the Ministry of Health, Labor and Welfare of Japan.

### Author details

[1]Department of Immunology, Graduate School of Medicine, University of the Ryukyus, Okinawa 903-0215, Japan. [2]Department of Pathology, Emory University School of Medicine, Atlanta, GA 30322, USA.

Received: 10 June 2013 Accepted: 12 November 2013
Published: 18 November 2013

### References

1. Ishii N, Takahashi T, Soroosh P, Sugamura K: **OX40-OX40 ligand interaction in T-cell-mediated immunity and immunopathology.** *Adv Immunol* 2010, **105**:63–98.
2. Croft M, Duan W, Choi H, Eun SY, Madireddi S, Mehta A: **TNF superfamily in inflammatory disease: translating basic insights.** *Trends Immunol* 2012, **33**:144–152.
3. Tanaka Y, Inoi T, Tozawa H, Yamamoto N, Hinuma Y: **A glycoprotein antigen detected with new monoclonal antibodies on the surface of human lymphocytes infected with human T-cell leukemia virus type-I (HTLV-I).** *Int J Cancer* 1985, **36**:549–555.
4. Miura S, Ohtani K, Numata N, Niki M, Ohbo K, Ina Y, Gojobori T, Tanaka Y, Tozawa H, Nakamura M, *et al*: **Molecular cloning and characterization of a novel glycoprotein, gp34, that is specifically induced by the human T-cell leukemia virus type I transactivator p40tax.** *Mol Cell Biol* 1991, **11**:1313–1325.
5. Ohshima Y, Tanaka Y, Tozawa H, Takahashi Y, Maliszewski C, Delespesse G: **Expression and function of OX40 ligand on human dendritic cells.** *J Immunol* 1997, **159**:3838–3848.
6. Baum PR, Gayle RB 3rd, Ramsdell F, Srinivasan S, Sorensen RA, Watson ML, Seldin MF, Clifford KN, Grabstein K, Alderson MR, *et al*: **Identification of OX40 ligand and preliminary characterization of its activities on OX40 receptor.** *Circ Shock* 1994, **44**:30–34.
7. Zingoni A, Sornasse T, Cocks BG, Tanaka Y, Santoni A, Lanier LL: **Cross-talk between activated human NK cells and CD4+ T cells via OX40-OX40 ligand interactions.** *J Immunol* 2004, **173**:3716–3724.
8. Kotani A, Hori T, Fujita T, Kambe N, Matsumura Y, Ishikawa T, Miyachi Y, Nagai K, Tanaka Y, Uchiyama T: **Involvement of OX40 ligand + mast cells in chronic GVHD after allogeneic hematopoietic stem cell transplantation.** *Bone Marrow Transplant* 2007, **39**:373–375.
9. Imura A, Hori T, Imada K, Kawamata S, Tanaka Y, Imamura S, Uchiyama T: **OX40 expressed on fresh leukemic cells from adult T-cell leukemia patients mediates cell adhesion to vascular endothelial cells: implication for the possible involvement of OX40 in leukemic cell infiltration.** *Blood* 1997, **89**:2951–2958.
10. Takasawa N, Ishii N, Higashimura N, Murata K, Tanaka Y, Nakamura M, Sasaki T, Sugamura K: **Expression of gp34 (OX40 ligand) and OX40 on human T cell clones.** *Jpn J Cancer Res* 2001, **92**:377–382.
11. Kondo K, Okuma K, Tanaka R, Zhang LF, Kodama A, Takahashi Y, Yamamoto N, Ansari AA, Tanaka Y: **Requirements for the functional expression of OX40 ligand on human activated CD4+ and CD8+ T cells.** *Hum Immunol* 2007, **68**:563–571.
12. Croft M: **Control of immunity by the TNFR-related molecule OX40 (CD134).** *Annu Rev Immunol* 2010, **28**:57–78.
13. Latza U, Durkop H, Schnittger S, Ringeling J, Eitelbach F, Hummel M, Fonatsch C, Stein H: **The human OX40 homolog: cDNA structure, expression and chromosomal assignment of the ACT35 antigen.** *Eur J Immunol* 1994, **24**:677–683.
14. Baum PR, Gayle RB 3rd, Ramsdell F, Srinivasan S, Sorensen RA, Watson ML, Seldin MF, Baker E, Sutherland GR, Clifford KN, *et al*: **Molecular characterization of murine and human OX40/OX40 ligand systems: identification of a human OX40 ligand as the HTLV-1-regulated protein gp34.** *EMBO J* 1994, **13**:3992–4001.
15. Weinberg AD, Evans DE, Thalhofer C, Shi T, Prell RA: **The generation of T cell memory: a review describing the molecular and cellular events following OX40 (CD134) engagement.** *J Leukoc Biol* 2004, **75**:962–972.
16. Compaan DM, Hymowitz SG: **The crystal structure of the costimulatory OX40-OX40L complex.** *Structure* 2006, **14**:1321–1330.
17. Imura A, Hori T, Imada K, Ishikawa T, Tanaka Y, Maeda M, Imamura S, Uchiyama T: **The human OX40/gp34 system directly mediates adhesion of activated T cells to vascular endothelial cells.** *J Exp Med* 1996, **183**:2185–2195.
18. Weinberg AD: **OX40: targeted immunotherapy–implications for tempering autoimmunity and enhancing vaccines.** *Trends Immunol* 2002, **23**:102–109.
19. Croft M, So T, Duan W, Soroosh P: **The significance of OX40 and OX40L to T-cell biology and immune disease.** *Immunol Rev* 2009, **229**:173–191.
20. Liu J, Ngai N, Stone GW, Yue FY, Ostrowski MA: **The adjuvancy of OX40 ligand (CD252) on an HIV-1 canarypox vaccine.** *Vaccine* 2009, **27**:5077–5084.
21. Tanaka R, Takahashi Y, Kodama A, Saito M, Ansari AA, Tanaka Y: **Suppression of CCR5-tropic HIV type 1 infection by OX40 stimulation via enhanced production of beta-chemokines.** *AIDS Res Hum Retroviruses* 2010, **26**:1147–1154.
22. Higashimura N, Takasawa N, Tanaka Y, Nakamura M, Sugamura K: **Induction of OX40, a receptor of gp34, on T cells by trans-acting transcriptional activator, Tax, of human T-cell leukemia virus type I.** *Jpn J Cancer Res* 1996, **87**:227–231.
23. Pichler K, Kattan T, Gentzsch J, Kress AK, Taylor GP, Bangham CR, Grassmann R: **Strong induction of 4-1BB, a growth and survival promoting costimulatory receptor, in HTLV-1-infected cultured and patients' T cells by the viral tax oncoprotein.** *Blood* 2008, **111**:4741–4751.
24. Kondo K, Okuma K, Tanaka R, Matsuzaki G, Ansari AA, Tanaka Y: **Rapid induction of OX40 ligand on primary T cells activated under DNA-damaging conditions.** *Hum Immunol* 2008, **69**:533–542.
25. Baba E, Takahashi Y, Lichtenfeld J, Tanaka R, Yoshida A, Sugamura K, Yamamoto N, Tanaka Y: **Functional CD4 T cells after intercellular molecular transfer of OX40 ligand.** *J Immunol* 2001, **167**:875–883.

26. Nam KO, Kang H, Shin SM, Cho KH, Kwon B, Kwon BS, Kim SJ, Lee HW: **Cross-linking of 4-1BB activates TCR-signaling pathways in CD8+ T lymphocytes.** *J Immunol* 2005, **174**:1898–1905.
27. Ma BY, Mikolajczak SA, Danesh A, Hosiawa KA, Cameron CM, Takaori-Kondo A, Uchiyama T, Kelvin DJ, Ochi A: **The expression and the regulatory role of OX40 and 4-1BB heterodimer in activated human T cells.** *Blood* 2005, **106**:2002–2010.
28. Taylor L, Bachler M, Duncan I, Keen S, Fallon R, Mair C, McDonald TT, Schwarz H: **In vitro and in vivo activities of OX40 (CD134)-IgG fusion protein isoforms with different levels of immune-effector functions.** *J Leukoc Biol* 2002, **72**:522–529.
29. Dannull J, Nair S, Su Z, Boczkowski D, DeBeck C, Yang B, Gilboa E, Vieweg J: **Enhancing the immunostimulatory function of dendritic cells by transfection with mRNA encoding OX40 ligand.** *Blood* 2005, **105**:3206–3213.
30. Tateyama M, Fujihara K, Ishii N, Sugamura K, Onodera Y, Itoyama Y: **Expression of OX40 in muscles of polymyositis and granulomatous myopathy.** *J Neurol Sci* 2002, **194**:29–34.
31. Muller N, Wyzgol A, Munkel S, Pfizenmaier K, Wajant H: **Activity of soluble OX40 ligand is enhanced by oligomerization and cell surface immobilization.** *FEBS J* 2008, **275**:2296–2304.
32. Barrios CS, Castillo L, Giam CZ, Wu L, Beilke MA: **Inhibition of HIV Type 1 replication by human T lymphotropic virus Types 1 and 2 Tax Proteins in Vitro.** *AIDS Res Hum Retroviruses* 2013, **29**:1061–1067.
33. Beilke MA: **Retroviral coinfections: HIV and HTLV: taking stock of more than a quarter century of research.** *AIDS Res Hum Retroviruses* 2012, **28**:139–147.
34. Tozawa H, Andoh S, Takayama Y, Tanaka Y, Lee B, Nakamura H, Hayami M, Hinuma Y: **Species-dependent antigenicity of the 34-kDa glycoprotein found on the membrane of various primate lymphocytes transformed by human T-cell leukemia virus type-I (HTLV-I) and simian T-cell leukemia virus (STLV-I).** *Int J Cancer* 1988, **41**:231–238.
35. Takahashi Y, Tanaka R, Yamamoto N, Tanaka Y: **Enhancement of OX40-induced apoptosis by TNF coactivation in OX40-expressing T cell lines in vitro leading to decreased targets for HIV type 1 production.** *AIDS Res Hum Retroviruses* 2008, **24**:423–435.
36. Tanaka Y, Inoi T, Tozawa H, Sugamura K, Hinuma Y: **New monoclonal antibodies that define multiple epitopes and a human-specific marker on the interleukin 2 receptor molecules of primates.** *Microbiol Immunol* 1986, **30**:373–388.
37. Inudoh M, Kato N, Tanaka Y: **New monoclonal antibodies against a recombinant second envelope protein of Hepatitis C virus.** *Microbiol Immunol* 1998, **42**:875–877.
38. Takahashi Y, Tanaka Y, Yamashita A, Koyanagi Y, Nakamura M, Yamamoto N: **OX40 stimulation by gp34/OX40 ligand enhances productive human immunodeficiency virus type 1 infection.** *J Virol* 2001, **75**:6748–6757.
39. Lee B, Tanaka Y, Tozawa H: **Monoclonal antibody defining tax protein of human T-cell leukemia virus type-I.** *Tohoku J Exp Med* 1989, **157**:1–11.
40. Tanaka R, Yoshida A, Murakami T, Baba E, Lichtenfeld J, Omori T, Kimura T, Tsurutani N, Fujii N, Wang ZX, *et al*: **Unique monoclonal antibody recognizing the third extracellular loop of CXCR4 induces lymphocyte agglutination and enhances human immunodeficiency virus type 1-mediated syncytium formation and productive infection.** *J Virol* 2001, **75**:11534–11543.

doi:10.1186/1743-422X-10-338
**Cite this article as:** Kasahara *et al.*: Natural OX40L expressed on human T cell leukemia virus type-I-immortalized T cell lines interferes with infection of activated peripheral blood mononuclear cells by CCR5-utilizing human immunodeficiency virus. *Virology Journal* 2013 10:338.

AIDS RESEARCH AND HUMAN RETROVIRUSES
Volume 29, Number 00, 2013

DOI: 10.1089/aid.2013.0109

# Genes Related to Antiviral Activity, Cell Migration, and Lysis Are Differentially Expressed in CD4$^+$ T Cells in Human T Cell Leukemia Virus Type 1-Associated Myelopathy/Tropical Spastic Paraparesis Patients

Mariana Tomazini Pinto,[1,2] Tathiane Maistro Malta,[1,2] Evandra Strazza Rodrigues,[1,2] Daniel Guariz Pinheiro,[1,3] Rodrigo Alexandre Panepucci,[1,4] Kelen Cristina Ribeiro Malmegrim de Farias,[1,2] Alessandra De Paula Sousa,[1] Osvaldo Massaiti Takayanagui,[4] Yuetsu Tanaka,[5] Dimas Tadeu Covas,[1,4] and Simone Kashima[1,2]

## Abstract

Human T cell leukemia virus type 1 (HTLV-1) preferentially infects CD4$^+$ T cells and these cells play a central role in HTLV-1 infection. In this study, we investigated the global gene expression profile of circulating CD4$^+$ T cells from the distinct clinical status of HTLV-1-infected individuals in regard to TAX expression levels. CD4$^+$ T cells were isolated from asymptomatic HTLV-1 carrier (HAC) and HTLV-1-associated myelopathy/tropical spastic paraparesis (HAM/TSP) patients in order to identify genes involved in HAM/TSP development using a microarray technique. Hierarchical clustering analysis showed that healthy control (CT) and HTLV-1-infected samples clustered separately. We also observed that the HAC and HAM/TSP groups clustered separately regardless of TAX expression. The gene expression profile of CD4$^+$ T cells was compared among the CT, HAC, and HAM/TSP groups. The paxillin (*Pxn*), chemokine (C-X-C motif) receptor 4 (*Cxcr4*), interleukin 27 (*IL27*), and granzyme A (*Gzma*) genes were differentially expressed between the HAC and HAM/TSP groups, regardless of TAX expression. The perforin 1 (*Prf1*) and forkhead box P3 (*Foxp3*) genes were increased in the HAM/TSP group and presented a positive correlation to the expression of TAX and the proviral load (PVL). The frequency of CD4$^+$FOXP3$^+$ regulatory T cells (Treg) was higher in HTLV-1-infected individuals. *Foxp3* gene expression was positively correlated with cell lysis-related genes (*Gzma*, *Gzmb*, and *Prf1*). These findings suggest that CD4$^+$ T cell activity is distinct between the HAC and HAM/TSP groups.

## Introduction

Human T cell leukemia virus type 1 (HTLV-1) was the first human retrovirus isolated.[1] HTLV-1 is the etiologic agent of HTLV-1-associated myelopathy/tropical spastic paraparesis (HAM/TSP),[2,3] adult T cell leukemia/lymphoma (ATLL),[4,5] and several inflammatory diseases including polymyositis, arthropathy, infective dermatitis, uveitis, and Sjögren's syndrome.[6–10]

The disease manifestations occur in 2–5% of infected individuals, and most individuals remain asymptomatic throughout life.[11,12] The mechanisms that lead to disease in infected patients are not fully understood and a number of factors such as genetic, demographic, environmental, and others have been suggested to contribute to disease development.[13–15]

HAM/TSP is a chronic progressive inflammatory disorder of the central nervous system (CNS) characterized by slow progressive spastic paraparesis, bladder disorder, weakness of the lower limbs, and less conspicuous sensory signs.[16] The clinical course of HAM/TSP varies among patients, but is more common in females.[17–19] Among several HTLV-1 genes, a transcriptional activator *Tax* may play a major role in the development of HAM/TSP, regulating multiple cellular responses by protein–protein interactions with various host cell factors. Moreover, *Tax* has been

[1]National Institute of Science and Technology in Stem Cell and Cell Therapy, Center for Cell-Based Therapy and Regional Blood Center of Ribeirão Preto, Ribeirão Preto, Brazil.
[2]Faculty of Pharmaceutical Sciences, University of São Paulo, Ribeirão Preto, Brazil.
[3]Department of Genetics, Faculty of Medicine of Ribeirão Preto, University of São Paulo, Ribeirão Preto, Brazil.
[4]Faculty of Medicine of Ribeirão Preto, University of São Paulo, Ribeirão Preto, Brazil.
[5]Department of Immunology, Graduate School of Medicine, University of the Ryukyus, Okinawa, Japan.

shown to disrupt cell cycle and DNA repair checkpoint, inactivate several tumor suppressors, and stimulate cell growth, while protecting against apoptosis.[20,21]

Although HTLV-1 is known to infect a wide range of human and nonhuman cells *in vitro*, HTLV-1 preferentially infects CD4 T cells, which become the main reservoir of HTLV-1.[22] It is also known that CD4 T cells predominate in the spinal cord mononuclear infiltrate of HAM/TSP patients.[23] In this way, in the early stages of the inflammatory process, cytokines such as interleukin (IL)-1$\alpha$, tumor necrosis factor (TNF)-$\alpha$, and interferon (IFN)-$\gamma$ are spontaneously secreted by these cells.[24] Thus, the potential contribution of CD4 T cells to the pathogenesis of this inflammatory disease as well as their expansion in HAM/TSP is more efficient due to the chronic antigenic stimulation that occurs in these individuals.[25,26]

The aim of this work was to identify genes differentially expressed among healthy control (CT), asymptomatic HTLV-1 carrier (HAC), and HAM/TSP patients in $CD4^+$ T cells isolated from these individuals. We showed that the global gene expression profile of circulating $CD4^+$ T cells from HTLV-1 individuals harboring distinct clinical status was altered regardless of TAX expression levels. Considering that most HTLV-1-infected individuals remain asymptomatic throughout life we explored genes that could be involved with HAM/TSP development.

## Materials and Methods

### *HTLV-1-infected individuals and healthy controls*

A total of 47 peripheral whole blood samples from HTLV-1-infected individuals were obtained and divided into two groups: the asymptomatic HAC group comprised of 26 individuals and the HAM/TSP group comprised of 21 symptomatic patients. Healthy controls (CT; $n=28$) had no previous or current infectious diseases caused by blood-borne pathogens. Samples of the CT individuals were recruited from the Regional Blood Center of Ribeirão Preto, São Paulo, Brazil, and HTLV-1-infected individuals were recruited from the Neurology Department of the Clinical Hospital of the Medical School of the University of São Paulo, Ribeirão Preto, São Paulo, Brazil.

The study was approved by the Institutional Ethics Committee (process number 3083/2007) and all individuals signed an informed consent before enrollment. All HTLV-1-infected individuals were evaluated for clinical status according to the criteria previously described for ATLL and HAM/TSP.[27] To be included in this study, the HTLV-1-infected individuals must have serological (rp21e-enhanced EIA; Cambridge Biotech) and molecular [conventional long-term repeat (LTR) and TAX polymerase chain reaction (PCR)] confirmation of the HTLV-1 infection.

All HTLV-1-infected and CT individuals included in this study presented negative serology for other relevant blood-borne pathogens including hepatitis B virus, hepatitis C virus, human immunodeficiency virus, Chagas disease, and syphilis. Hemogram and CD4 and CD8 T cell counts were performed for all individuals.

### *Molecular diagnosis and proviral load*

Genomic DNA was extracted using the Super Quick Gene DNA isolation kit (Analytical Genetic Testing Center–AGTC, Denver, CO) following the manufacturer's instructions. The in house PCR (LTR and Tax regions) tests were as previously described.[28] The proviral load was quantified using TaqMan Universal PCR Master Mix (Applied Biosystems, Foster City, CA) and specific primers of the HTLV-1 Tax region. The reaction was composed of 500 ng of genomic DNA, 6.25 $\mu$l TaqMan Universal PCR Master Mix, 5 $\mu$M of the forward primer (5'-CCC ATC GAT GGA CGC GT-3'), 5 $\mu$M of the reverse primer (5'-CTC CTT CCC CAC CCA GAG AA-3'), and 5 $\mu$M of the specific probe (5'-FAM-CGG CTC AGC TCT ACA G-3'-MGB). Human $\beta$-actin (*Actb*) was used as the endogenous control (TaqMan Gene Expression Assays–Hs03023880_g1) (Applied Biosystems, Foster City, CA). Serially diluted (from $10^5$ to $10^1$ copies) DNA from HTLV-1-infected MT-2 cells was used for generating standard curves for the HTLV-1 *Tax* gene. Real-time PCR was performed in duplicate for all DNA standards and samples using the ABI Prism 7500 Sequence Detection System (Applied Biosystems, Foster City, CA) with the following conditions: 50°C for 2 min, 95°C for 10 min, followed by 40 cycles at 95°C for 15 s/60°C for 1 min. Proviral load was calculated using the following formula: (copy number of *Tax*)/(copy number of $\beta$-actin)$\times 2 \times 100{,}000$.

### *$CD4^+$ T cell isolation*

Peripheral blood mononuclear cells (PBMCs) were isolated by Ficoll Hypaque PLUS (GE Healthcare Bio-Sciences AB, Uppsala, Sweden). $CD4^+$ T cells were then isolated from PBMCs by positive selection using immunomagnetic beads (Miltenyi Biotec GmbH, Bergisch Gladbach, Germany) and the purity of the $CD3^+CD4^+$ T cells was confirmed by flow cytometry using the surface markers anti-CD4-FITC and anti-CD3-PE (FACSCalibur, Becton & Dickinson, San Jose, CA).

### *Microarray analysis*

Twelve samples underwent microarray analysis, as follows: four CT, four HAC, and four HAM/TSP samples. The criterion used to select HTLV-1-infected individuals was TAX expression levels in PBMCs as assessed by flow cytometry. Two samples had high TAX expression and two samples had low TAX expression for both groups (Table 1). All samples had purity above 90%. We considered high TAX expression levels those with values higher than 1.39% (obtained by the median of all HTLV-1-infected individuals). In these samples, proviral load correlated with TAX expression (data not shown). Total RNA was isolated with *TRIzol Reagent* (Invitrogen, Carlsbad, CC) and purified with the RNeasy Mini Kit (Qiagen, Hilden, Germany).

One color microarray-based gene expression analysis (Quick Amp Labeling) (Agilent, Santa Clara, CA) was done according to the manufacturer's instructions. The microarray was scanned with an Axon GenePix 4000B Microarray Scanner (Molecular Devices, Sunnyvale, CA) and data were processed using Feature Extraction software version 9.5.1 (Agilent, Santa Clara, CA). Quality control and array normalization were done in R environment at (www.r-project.org) with the Agi4x44PreProcess bioconductor package (http://bioconductor.org/). Normalization and filtering were done following the Agi4x44-Pre-Process instructions. Genes differentially expressed were identified based on a $\log_2$-fold change of 2-fold at least and a statistically significant level using the *t*-test ($p$ value $< 0.005$). The expression profiles of the differentially expressed genes were determined by cluster analysis based on the k-means method using Euclidean distance (Genesis 1.7.5). Ingenuity

TABLE 1. DESCRIPTIVE CHARACTERISTICS OF HUMAN T CELL LEUKEMIA VIRUS TYPE 1-INFECTED INDIVIDUALS INCLUDED IN THE MICROARRAY ANALYSIS

| *Clinical status* | *Gender* | *Age (years)* | *TAX expression in CD4$^+$ (%)* | *Leukocytes global count (cells/mm$^3$)* | *Absolute count of CD4/CD8 (reason)* | *Purity (%) CD4$^+$* |
|---|---|---|---|---|---|---|
| HAC 08 | F | 26 | 8.87 | 5,600 | 1251/760 (1.65) | 96.87 |
| HAC 16 | F | 55 | 0.14 | 7,100 | 708/237 (2.98) | 95.22 |
| HAC 19 | F | 33 | 0.16 | 4,800 | 1166/274 (4.26) | 95.02 |
| HAC 21 | M | 46 | 3.32 | 6,700 | 1225/558 (2.20) | 95.31 |
| HAM 01 | F | 55 | 0.44 | 6,000 | 717/378 (1.90) | 94.94 |
| HAM 09 | M | 64 | 3.66 | 3,700 | 468/355 (1.32) | 96.31 |
| HAM 14 | F | 61 | 2.97 | 6,000 | 665/256 (2.60) | 93.82 |
| HAM 17 | F | 55 | 0.54 | 8,600 | 579/272 (2.13) | 93.62 |

Characteristics according to gender, age, TAX expression in CD4$^+$ T cells, leukocyte global count, absolute count of CD4/CD8, and purity of CD4$^+$ T cells.

HTLV-1, human T cell leukemia virus type 1; HAC, asymptomatic HTLV-1 carrier; HAM/TSP, HTLV-1-associated myelopathy/tropical spastic paraparesis; F, female; M, male.

Pathway Analysis (IPA) was used to evaluate the microarray data for relevant biological themes within the differentially expressed genes. Microarray data have been deposited in the NCBI Gene Expression Omnibus (www.ncbi.nlm.nih.gov/geo/) (GEO ID: GSE38537).

### *Real-Time RT-PCR*

Total RNA was reverse transcribed (RT) using the High Capacity cDNA Reverse Transcription Kit (Applied Biosystems, Foster City, CA) following the manufacturer's instructions. Differentially expressed genes were validated by a real-time PCR technique using TaqMan Gene Expression Assays (Applied Biosystems, Foster City, CA). The PCR amplification and fluorescence data collection were performed with ABI 7500 Sequence Detection (Applied Biosystems, Foster City, CA).

The following genes were validated: granzyme A (*Gzma*) (Hs00196206_m1), granzyme B (*Gzmb*) (Hs00188051_m1), perforin 1 (*Prf1*) (Hs00169473_m1), chemokine (C-X-C motif) receptor 4 (*Cxcr4*) (Hs00237052_m1), paxillin (*Pxn*) (Hs01104424_m1), forkhead box P3 (*Foxp3*) (Hs01085834_m1), and interleukin 27 (*IL27*) (Hs00377366_m1).

The housekeeping genes $\beta$-actin (*Actb*) (4326315E), glyceraldehyde-3-phosphate dehydrogenase (*Gapdh*) (4310884-E), $\beta_2$-microglobulin (*B2m*) (4333766-0710013), and ribosomal protein L13a (*Rpl13a*) (185720330-7)[29] were used to normalize sample loading (Applied Biosystems). The $2^{-\Delta\Delta Ct}$ method was used to calculate the relative expression levels.[30] All the reactions were duplicated.

### *Flow cytometry analysis*

TAX expression was detected in PBMCs. Cells were cultured in RPMI 1640 (Sigma-Aldrich, Saint Louis, MO) containing 10% fetal calf serum (HyClone, Logan, UT) and 20 nM concanamycin A (Sigma-Aldrich, St. Louis, MO) for 12 h under 5% $CO_2$ at 37°C.

A total of $2.5\times10^5$ cells were stained for surface markers anti-CD4-PE, anti-CD8-PerCP, and anti-CD3-APC (Becton & Dickinson, San Jose, CA). For intracellular analysis, cells were fixed with 4% paraformaldehyde in phosphate-buffered saline (PBS) for 20 min.

Fixed cells were washed with PBS containing 4% normal goat serum (NGS) (Sigma) and then washed with PBS containing 0.1% Triton X-100 (Sigma) for 10 min at room temperature. Permeabilized cells were washed and resuspended in PBS/4% NGS containing an anti-HTLV-I TAX monoclonal antibody (mAb) (Lt-4; $IgG_3$), antihuman-PRF1-clone $\delta$G9, antihuman-GZMB-clone GB11 (Becton & Dickinson, San Jose, CA), or an isotype control mAb (Southern Biotechnology Associates, Birmingham, AL) for 30 min at room temperature. For intracellular TAX detection, cells were stained with Alexa Fluor 488-labeled goat antimouse $IgG_3$ (Invitrogen, Carlsbad, CA) for 30 min at room temperature.

For CXCR4 detection, 150 $\mu$l of whole blood and 5 $\mu$l of antibodies anti-CD4-FITC, anti-CD3-PerCP, and anti-human-CXCR4-PE-clone 12G5 (Becton & Dickinson, San Jose, CA) were used. The reaction was incubated for 15 min and then 1 ml of FACS Lysing Solution (1×) (Becton & Dickinson, San Jose, CA) was added. All samples were analyzed on a FACSCalibur flow cytometer (Becton & Dickinson, San Jose, CA).

For FOXP3 expression, isolated PBMCs were immunostained with a saturating concentration of anti-CD25-FITC, anti-CD4-PerCP, and anti-CD3-APC for 15 min at room temperature. Then 1 ml of FACS Lysing Solution (1×) (Becton & Dickinson, San Jose, CA) was added. Cells were permeabilized using FACS Permeabilizing Solution 2 (Becton & Dickinson, San Jose, CA) and stained intracellularly for 10 min with antihuman-FOXP3-PE-clone 259/C7. Finally, the cells were washed with PBS and analyzed on a FACSCalibur flow cytometer (Becton & Dickinson, San Jose, CA).

### *Statistical analysis*

Data were analyzed in GraphPad PRISM, version 5.01 (GraphPad software California) using nonparametric statistical tests. The results from quantitative PCR and flow cytometry were analyzed using a one-tailed Mann–Whitney *U*-test. The correlations among different parameters were assessed with Spearman's rank correlation. In all these cases, statistically significant differences were considered when $p$ values were $\leq 0.05$.

## Results

### *Clinical and demographic data*

The clinical and demographic data of patients are shown in Table 2. A total of 75 individuals were included in our study of

Table 2. Clinical and Viral Characteristics of Human T Cell Leukemia Virus Type 1-Infected Individuals and Healthy Controls Enrolled in the Study

| | *CT* (n=*28*) | *HAC* (n=*26*) | *HAM/TSP* (n=*21*) |
|---|---|---|---|
| Age | 46.5 | 42.9 | 54.9 |
| Gender (F:M) | 2.5 | 1.4 | 3.2 |
| Proviral load mean (copy number/$10^5$ cells)[a] | — | 6,586 | 12,233[b] |
| TAX expression (%) | — | 1.1 | 2.5[b] |
| Leukocyte global count (cells/$mm^3$) | 7,225 | 6,816 | 6,771 |
| CD4/CD8 ratio | 2.21 | 2.10 | 2.98 |

[a]Proviral load copy number/$10^5$ cells.
[b]$p \leq 0.01$ (unpaired $t$ test).
Table shows average values. CT, healthy controls; HAC, asymptomatic HTLV-1 carrier; HAM/TSP, HTLV-1-associated myelopathy/tropical spastic paraparesis; F:M, female/male ratio.

which 51 were female (68%). The mean onset age in the HAM/TSP group was 54.9 years (ranging from 37 to 74 years), which was higher than the CT (mean 46.5 years) and HAC groups (mean onset age 42.9 years). Proviral load was increased (1.8×) in the HAM/TSP group ($p=0.0024$) when compared to the HAC group (data not shown). TAX expression positively correlated with proviral load ($r=0.7433$; $p<0.0001$) and the percentage of $CD4^+$ T cells expressing TAX was higher in the HAM/TSP group (data not shown). No differences were observed in leukocyte global counts and CD4/CD8 ratio among groups.

### *Global gene expression in $CD4^+$ T cells*

The microarray platform was tested with 12 individual samples divided according to patients' clinical status and TAX expression as follows: CT ($n=4$), HAC ($n=4$; composed of two samples with high TAX expression and two with low TAX expression), and HAM/TSP group ($n=4$; composed of two samples with high TAX expression and two with low TAX expression). We used a hierarchical clustering to group samples according to their gene expression levels. Dendrogram analysis showed that clustering of $CD4^+$ T cells allowed a clear separation between CT and HTLV-1-infected individuals. We also observed that the HAC and HAM/TSP groups clustered apart (Fig. 1). However, HTLV-1 $CD4^+$ T cell clustering did not correlate with TAX protein expression.

### *Gene expression analysis*

A total of 45,015 probes were screened by the Agilent microarray platform. The background correction, filtering, normalization, and summarization of probes were performed using the Agi4x44PreProcess package resulting in 27,061 distinct probes, from which only 19,668 remained in the subsequent analysis after the filtering of probes annotated as ribosomal proteins, or in sexual chromosomes or unannotated probes. In microarray analysis, genes were considered differentially expressed on the basis of a $\log_2$-fold change of 2-fold at least and a statistically significant level using a $t$-test ($p$ value < 0.005). We found 201 differently expressed genes between the CT and HAC groups (166 genes down-regulated and 35 genes up-regulated in the HAC group), 244 genes between the CT and HAM/TSP groups (165 genes down-regulated and 79 genes up-regulated in the HAM/TSP group), and 68 genes between the HAC and HAM/TSP groups (66 genes down-regulated and 2 genes up-regulated in the HAM/TSP group) (Fig. 2A–C). Additionally, we determined which genes were in common among these groups (Fig. 2D). Supplementary Tables S1–S6 (Supplementary Data are available online at www.liebertpub.com/aid) SUPPL TABLES S1–S6 list all genes shown in Venn diagrams. Only one differentially expressed gene (*Tmeff2*) was observed between HAM/TSP vs. HAC and CT vs. HAC analysis. We did not select this gene to study because it was not associated with inflammatory and infectious disease.

### *Genes related to cell migration were up-regulated in the HAM/TSP group*

Eighty-four differentially expressed genes in common were observed between CT vs. HAC and CT vs. HAM/TSP analysis, with most of them overexpressed in the CT group (Fig. 3A). *In silico* analysis demonstrated that six genes, namely paxillin (*Pxn*), CD4, *Ptk2b*, *Ccl5*, *Tnf*, and *Gh1*, were represented in a network that is related to apoptosis, inflammatory and immunological diseases, cell–cell interaction, movement and repair of cell functions, and cell migration (Fig. 3B). The *Pxn* gene was also present in the *Cxcr4* pathway that is responsible for cell migration. The global gene expression profile showed that *Pxn* was increased in the CT group compared to the HAC (fold change: 5.1, $p=0.0913$) and HAM/TSP groups (fold change: 8.2, $p=0.0002$). The *Pxn* and *Cxcr4* genes were validated by quantitative real-time PCR (qPCR) and both of them showed an increased expression in HAM/TSP individuals (Fig. 3C). The level of *Pxn* gene expression was increased in HTLV-1-infected individuals ($p=0.0022$) (data not shown). Moreover, the CXCR4 protein was analyzed by flow cytometry among the groups, but no statistically significant difference was observed (data not shown).

### *IL27 gene expression is higher in HAC individuals*

Forty-two differentially expressed genes exclusive between HAC and HAM/TSP analysis were found. These genes were related to cell–cell interaction, inflammatory response, and cellular immune response, which include interleukin 27 (*IL27*). A global gene expression profile showed that *IL27* was increased in the HAC group compared to the HAM/TSP groups (fold change: 5.24). This result was validated by qPCR in which levels of *IL27* gene expression were higher in the HAC group compared to the HAM/TSP group ($p=0.0392$) (Fig. 4A). Additionally, *IL27* gene expression was higher in HTLV-1-infected individuals compared to the CT group ($p=0.0019$) (data not shown).

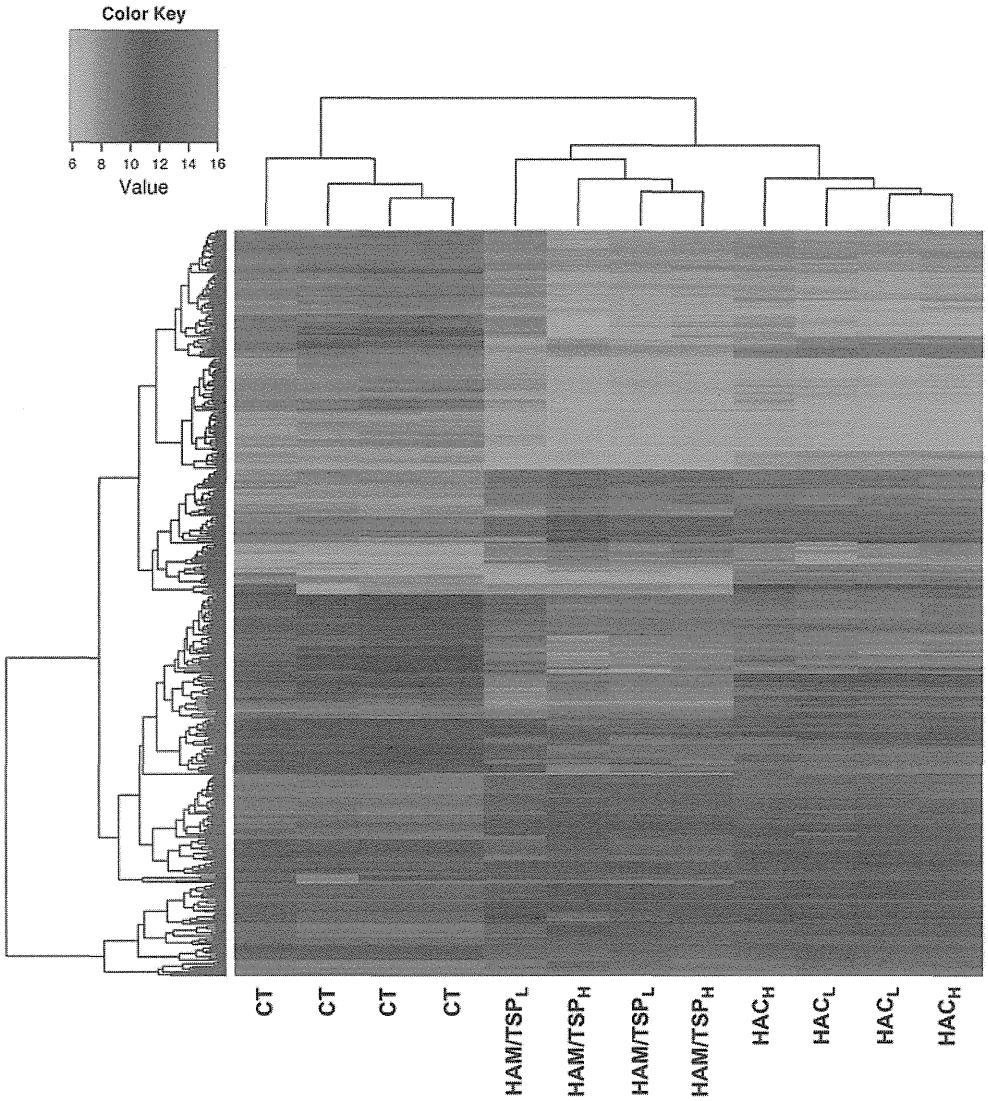


**FIG. 1.** Gene expression heat map and dendrogram of $CD4^+$ T cells. Hierarchical clustering of all detected genes showed a clear clustering of CT, HAC, and HAM/TSP samples using an average linkage and Euclidian distance metric. Expression values from all microarrays were used to group transcription profiles according to their similarities among groups. The heat map shows a distinct gene expression profile in the three groups analyzed. Rows indicate the relative levels of expression for a single gene, and columns show the expression level for a single sample. Green and red colors indicate those genes with lower and higher expression levels, respectively. CT, healthy control; HAC, asymptomatic human T cell leukemia virus type 1 (HTLV-1) carrier; HAM/TSP, HTLV-1-associated myelopathy/tropical spastic paraparesis; $HAC_L$, low TAX expression; $HAC_H$, high TAX expression; $HAM/TSP_L$, low TAX expression; $HAM/TSP_H$, high TAX expression.

### *HAM/TSP $CD4^+$ T cells had higher expression of cell lysis-related genes*

The 25 differentially expressed genes in common between CT vs. HAM/TSP and HAM/TSP vs. HAC analyses were evaluated for their participation in signaling pathways and only three pathways were observed, among them granzyme A (*Gzma*). Although the *Gzma* gene was not in accordance with the parameters of analyses (2-fold and $p$ value 0.005), the global gene expression profile showed that *Gzma* was increased in the HAM/TSP group compared to the CT (fold change: 1.9, $p=0.0038$) and HAC groups (fold change: 1.9, $p=0.0071$). For that reason, this gene was selected for validation due to it being poorly studied on $CD4^+$ T cells infected by HTLV-1 and due to its possible involvement in HAM/TSP development.

The levels of *Gzma* gene expression were evaluated (Fig. 4B) and we observed an increase in the HAM/TSP group compared to the CT ($p=0.0038$) and HAC ($p=0.0071$) groups. Therefore, we suggest that other genes related to cell lysis could also be increased in the HAM/TSP group, such as *Gzmb* and *Prf1*. Therefore, we analyzed *Gzmb* and *Prf1* gene expression (Fig. 4C and D). The HAM/TSP group showed higher gene expression levels of *Prf1* compared to the CT ($p<0.0001$) and HAC ($p=0.0037$) groups. *Prf1* gene expression was increased ($p=0.003$) in HTLV-1-infected individuals when compared to the CT group (data not shown). No difference was observed in gene expression level of *Gzmb* among the three groups. GZMB and PRF1 proteins were analyzed by flow cytometry; however, no difference was observed among the CT, HAC, and HAM/TSP groups (data not shown).

It was reported that regulatory T cells (Treg) have cytolytic capacity and perforin/granzyme pathways are required for this activity.[31] *Foxp3* gene expression, one of the main Treg cell markers, was also evaluated (Fig. 4E). As expected, we notice an overexpression of *Foxp3* in the HAM/TSP group compared to the CT and HAC groups ($p=0.0003$ and $p=0.0016$, respectively). *Foxp3* gene expression was increased in HTLV-1-infected individuals ($p=0.0128$) compared to CT individuals (data not shown).

### *The lysis-related genes were correlated with Foxp3 expression and Prf1 and Foxp3 genes were correlated with TAX expression and proviral load (PVL)*

Since the *Gzma*, *Prf1*, and *Foxp3* genes were shown to have an increased expression in HAM/TSP individuals, we thought these genes could be correlated. We performed

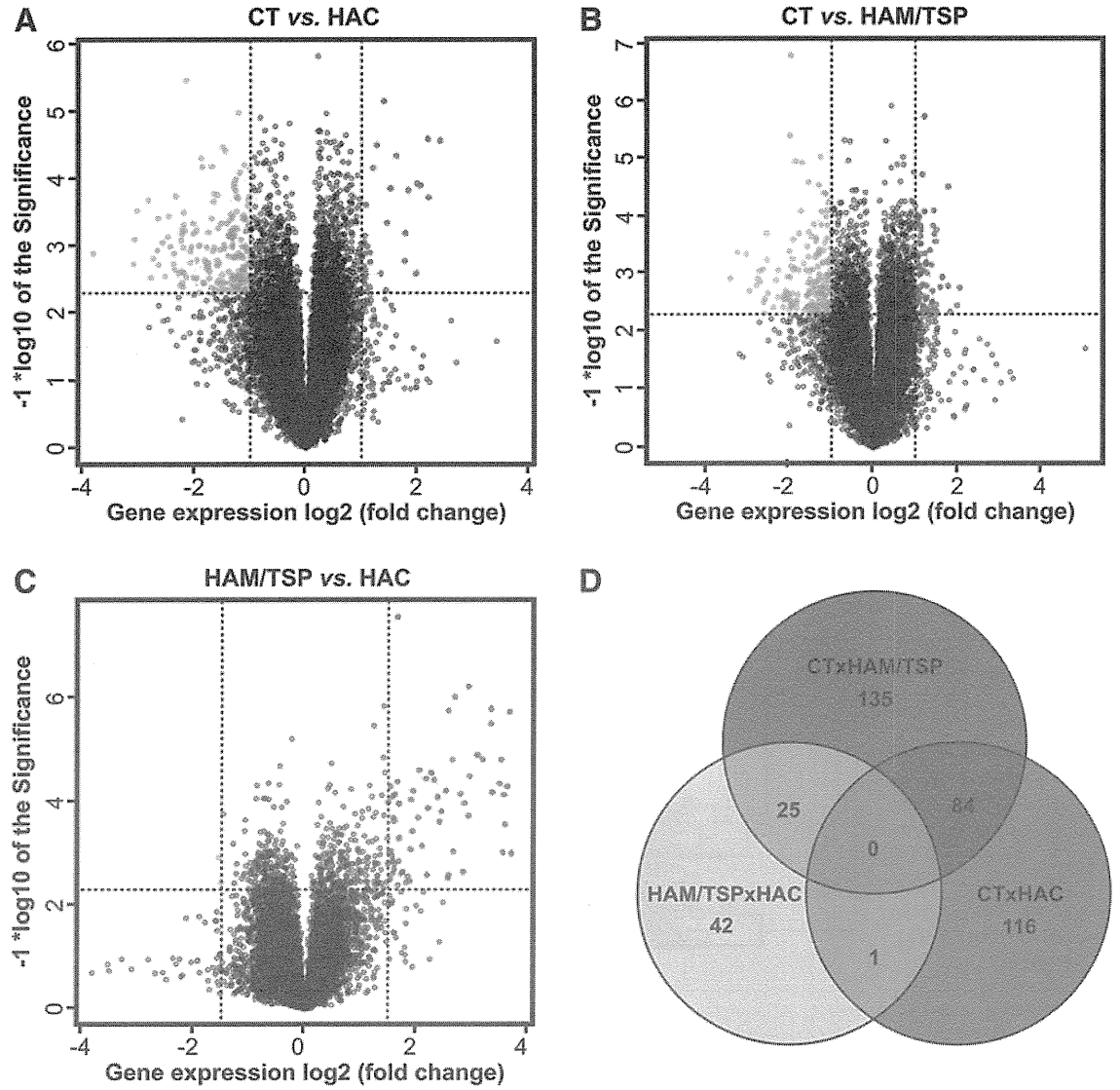


**FIG. 2.** Differently expressed genes among the CT, HAC, and HAM/TSP groups. Differently expressed genes between the CT and HAC groups **(A)**, CT and HAM/TSP groups **(B)**, and HAC and HAM/TSP groups **(C)** represented by Volcano Plot. Overexpressed genes right are on the upper side and underexpressed genes are on the upper left side. Dots in the middle of the figure represent genes for which the expression showed no statistical difference (Euclidian distance – complete linkage). **(D)** Venn diagram representation of differentially expressed genes. Venn diagrams showed an overlap of genes that are commonly expressed in the three clinical states. CT, healthy control; HAC, asymptomatic HTLV-1 carrier; HAM/TSP, HTLV-1-associated myelopathy/tropical spastic paraparesis.

Spearman's correlation test and verified that the *Gzma*, *Gzmb*, and *Prf1* genes were positively correlated with *Foxp3* gene expression (Fig. 5A–C). We evaluated whether all the genes analyzed in this study (*Pxn*, *Cxcr4*, *IL27*, *Gzma*, *Gzmb*, *Prf1*, and *Foxp3* genes) were correlated with TAX viral protein expression and PVL values. However, only the *Prf1* and *Foxp3* genes presented a positive correlation with TAX expression and the PVL (Fig. 5D–G).

### *$CD4^+FOXP3^+$ cell percentage was increased in HTLV-1-infected individuals*

The phenotype $CD4^+FOXP3^+$ is used to identify a major population of Tregs.[32] Thus we analyzed $CD4^+FOXP3^+$ cell percentage in the CT, HAC, and HAM/TSP groups. The percentage of $CD4^+FOXP3^+$ cells was consistently higher ($p=0.0017$) in HTLV-1-infected individuals than in the CT group (Fig. 5H). The analyses have revealed an increase ($8\times$) in the HAC group compared to the CT group ($p=0.0016$) and an increase ($3\times$) in the HAM/TSP group compared to the CT group ($p=0.0128$) (data not shown).

## Discussion

We demonstrated that the gene expression profile in $CD4^+$ T cells differs between the HAC and HAM/TSP groups regardless of TAX expression. It has been well established that HAM/TSP individuals have an HTLV-1 PVL and TAX expression higher than asymptomatic individuals.[33–36] These findings suggest that the risk of HTLV-1 inflammatory diseases strongly correlates with PVL.[37] Here, we demonstrated that PVL and TAX expression of $CD4^+$ T cells positively